Food & Function

Germinated chickpea protein ficin hydrolysate and its peptides inhibited glucose uptake and affected the bitter receptor signaling pathway in vitro

Journal:	*Food & Function*
Manuscript ID	FO-ART-04-2023-001408.R1
Article Type:	Paper
Date Submitted by the Author:	30-Jul-2023
Complete List of Authors:	Chandrasekaran, Subhiksha; University of Illinois at Urbana-Champaign Department of Food Science and Human Nutrition Gonzalez de Mejia, Elvira; University of Illinois at Urbana-Champaign Department of Food Science and Human Nutrition, ;

1 Germinated chickpea protein ficin hydrolysate and its peptides inhibited glucose uptake and affected
2 the bitter receptor signaling pathway *in vitro*
3
4 Subhiksha Chandrasekaran and Elvira Gonzalez de Mejia
5 Department of Food Science and Human Nutrition, University of Illinois at Urbana-Champaign,
6 Urbana, IL USA 61801
7
8 Corresponding author: Elvira Gonzalez de Mejia, 228 ERML; 1201 West Gregory Dr., Urbana, IL
9 61801; phone, 217-244-3196; edemejia@illinois.edu; https://orcid.org/0000-0001-7426-9035

10 Abstract

11 The objective of this study was to evaluate germinated chickpea protein hydrolysate (GCPH) *in vitro*
12 for its effect on markers of type 2 diabetes (T2D) and bitter taste receptor expression in intestinal
13 epithelial cells. Protein hydrolysate was obtained using ficin, and the resulting peptides were sequenced
14 using LC-ESI-MS/MS. Caco-2 cells were used to determine glucose uptake and extra-oral bitter receptor
15 activation. Three peptides, VVFW, GEAGR, and FDLPAL, were identified in legumin. FDLPAL was the
16 most potent peptide in molecular docking studies with a DPP-IV energy of affinity of -9.8 kcal/mol.
17 GCPH significantly inhibited DPP-IV production by Caco-2 cells (IC_{50} = 2.1 mM). Glucose uptake was
18 inhibited in a dose-dependent manner (IC_{25} = 2.0 mM). A negative correlation was found between
19 glucose uptake and PLCβ2 expression in Caco-2 cells (R value, -0.62). Thus, GCPH has the potential to
20 be commercialized as a functional ingredient.

21 Keywords: bitterness; chickpea; *Cicer arietinum;* dipeptidyl peptidase IV; diabetes; germination;
22 protein; α-glucosidase

23

24 1. Introduction

25 Chickpea is the second most produced legume globally, with 15.1 million tons produced worldwide as
26 of 2021 [1]. Steady growth in the consumption of alternative proteins allows for the increased use of
27 chickpea and its proteins [2]. Among different processing methods, germination is a low-cost option that
28 improves nutrient digestibility by activating endoproteases [3]. The biological potential of germinated
29 chickpeas has been well documented. Germinated chickpeas have antioxidant, antihypertensive,
30 antihyperlipidemic, antiadipogenic, and antidiabetic properties [4–6].

31 Bioactive peptides are released through protein hydrolysis [7], and chickpea protein hydrolysates have
32 multiple bioactive properties, such as antioxidant, anti-inflammatory, antihypertensive, and
33 antihyperlipidemic activities [8–11]. Therefore, germination, in combination with protein hydrolysis, may
34 enhance the release of bioactive peptides.

35 Type 2 diabetes (T2D) is characterized by a reduced response of pancreatic β-cells to insulin secretion
36 [12]. The International Diabetes Federation estimated that 374 million people were at risk of developing
37 T2D in 2019. While there is extensive knowledge of the antidiabetic potential of chickpea protein
38 hydrolysates in biochemical models [13], evaluation of germinated chickpea protein hydrolysate (GCPH) is
39 limited.

40 The expression of the glucose transporters sodium/glucose cotransporter 1 (SGLT1) and glucose
41 transporter 2 (GLUT2) has been confirmed in Caco-2 cells [14]. Glucose transporter inhibitors are
42 commercially utilized as therapeutic agents for the management of T2D to control glucose homeostasis in
43 the body [15]. Caco-2 cells have also been established as a model for studying dipeptidyl peptidase-IV
44 (DPP-IV) production in enterocytes. DPP-IV inhibits the action of glucagon-like peptide 1 (GLP-1),
45 which regulates glucose homeostasis [16]. Commercially available therapeutic agents such as sitagliptin
46 targeting DPP-IV are used to manage and treat T2D.

47 Additionally, Caco-2 cells have been used to model the activity of sucrase-isomaltase (SI)[17]. SI is
48 responsible for digesting sucrose, maltose and isomaltose in the gut, and further yielding fructose and

glucose. SI is responsible for nearly 100% of sucrose digestion, and 60-80% of maltose digestion. Reducing SI activity reduces glucose available for absorption.

Recently, extraoral bitter receptors identified in the gut have been found to play a therapeutic role in T2D management [18]. Specifically, increased GLP-1 production is associated with bitter taste receptor activation [19]. Other markers associated with T2D, such as DPP-IV inhibition, glucose uptake and SI activity have not been explored extensively with regard to their relationship with bitter taste receptor activation. However, reducing bitterness of a pea protein isolate has been shown to significantly reduce DPP-IV activity in biochemical models [20]. Additionally, both bitter receptor activation and glucose uptake share common markers, such as PLCβ2 and TRPM5, but to the best of our knowledge, the relationship between the two needs more research [21].

Enzymatic hydrolysis of plant-based proteins has been shown to both increase and decrease the bitter taste of the hydrolysate, depending on the hydrolysis conditions and the composition of the isolate [22]. While there is some data regarding the bitter taste of peptides and plant-based protein hydrolysates, there is limited data on the effect of its bitterness on markers of T2D in *in vitro* systems. It is therefore necessary to describe the relationship between bitterness and health-related potential.

Therefore, the objective of this study was to evaluate the effects of germinated chickpea protein ficin hydrolysate and its peptides on glucose uptake, DPP-IV, α-glucosidase, as well as analyze bitter taste receptor expression *in vitro*. This study is unique in discovering the mechanism of action of GCPH and the effect of some of its peptides produced using ficin on well-established markers of T2D and the potential role of bitter receptor activation in the process.

2. Materials and methods

2.1. Materials

The United States Department of Agriculture (Washington, USA) provided the Billy bean variety of Kabuli chickpea. Caco-2 (ATCC® HTB-37) cells were purchased from the American Type Culture Collection (ATCC, Manassas, VA, USA). Eagle's minimum essential medium and Dulbecco's modified

74 eagle medium was purchased from Corning (NY, USA). Fetal bovine serum was purchased from Grand
75 Island Biological Company (GIBCO, Grand Island, NY, USA). Protein reagents A and B, 2x Laemmli
76 sample buffer, 10x Tris/Glycine/SDS buffer, mini-PROTEAN ® TGX pre-cast gels (4-20%, 10 well-
77 comb, 30 μL) and Precision Plus Protein ™ Dual Xtra standard were purchased from BioRad (Hercules,
78 CA, USA). Antibiotics penicillin and streptomycin were purchased from Lonza (Basel, Switzerland).
79 Pure peptides used were synthesized by GenScript (Piscataway, NJ, USA) and had a purity of 95%,
80 verified using UPLC by the company.
81 DPP-IV (EC 3.4.14.5) was used to evaluate anti-diabetic potential biochemically. SGLT1 polyclonal
82 antibody from rabbit (0.26 mg/mL), T2R4 (bitter taste receptor 4) polyclonal antibody from rabbit (1
83 mg/mL), PLCβ2 polyclonal antibody from rabbit (0.71 mg/mL), TRPM5 polyclonal antibody from rabbit
84 (0.5 mg/mL) were purchased from Thermofisher. The epitopes of the antibodies were 252-612 (SGLT1),
85 31-60 (GLUT2), 229-278 (T2R14), 61-85 (T2R4), 1021-1108 (TRPM5), within the C-terminus region.
86 All other reagents from purchased from Sigma Aldrich unless indicated otherwise (St. Louis, MO, USA).
87 Experiments were carried out to evaluate the effect of germinated chickpea protein hydrolysate
88 (GCPH) on antidiabetic markers and bitter taste receptor expression in Caco-2 cells. Chickpeas were
89 germinated at 30℃ with 80% RH, protein was isolated at pH 4.5, enzymatic hydrolysis of chickpea
90 protein was carried out with ficin at 1:10 E/S ratio, 30 min hydrolysis time. Following this, germinated
91 chickpea protein hydrolysate was used for peptide sequencing liquid chromatography electrospray
92 ionization-mass spectrometry/mass spectrometry (LC-ESI-MS/MS) to understand composition and
93 identify peptides of interest. Identified peptides from storage proteins were used in molecular docking
94 with markers dipeptidyl peptidase-IV (DPP-IV), sucrase-isomaltase (SI), SGLT1, GLUT2, T2R4 and
95 T214. Biochemical assays for DPP-IV and α-glucosidase inhibition were done with GCPH and pure
96 peptides. Finally, *in vitro* assays with Caco-2 cells, including DPP-IV inhibition, SI inhibition, and
97 western blots with cell lysates to evaluate SGLT1, GLUT2, T2R4, T2R14, PLCβ2 and TRPM5
98 expression were done.

99 *2.2 Germination of chickpea*

100 A previously established protocol was followed [23]. Six days of germination was chosen based on a
101 previous experimental model using response surface design, which considered the role of germination
102 time, hydrolysis time and enzyme/substrate ratio. Chickpeas were germinated at 30℃ and at 80% RH.
103 Germinated chickpeas were freeze-dried for further analysis (FreezerZone ®, LabConco, Kansas,
104 US).

105 *2.3 Isolation and protein quantification of germinated chickpea protein*

106 A previously established protocol was followed [23]. Chickpea protein was isolated using the isoelectric
107 point (pH 4.5). The protein isolate was freeze-dried for further analysis. Soluble protein content was
108 determined using the DC protein assay kit according to the manufacturer's protocol (Bio-Rad, Hercules,
109 California, USA). The absorbance was measured at 540 nm using a Synergy2 multiwell plate reader
110 (BioTek instruments, Winooski, Vermont, USA).

111 *2.4 Hydrolysis and sodium dodecyl sulphate-polyacrylamide gel electrophoresis of germinated*
112 *chickpea protein*

113 The optimum conditions from our previous study were used [23] for germinated chickpea protein
114 hydrolysis. Based on a previous response surface design model, ficin was found to produce optimum
115 production conditions for a chickpea protein hydrolysate. The optimum conditions from our previous
116 study[23], specifically 30 min hydrolysis and 1:10 E/S ratio, were used for enzymatic hydrolysis.
117 Additionally, to the best of our knowledge, ficin has not been explored significantly in producing
118 chickpea protein hydrolysate, and has been proven to produce bioactive peptides from other protein
119 isolates [24].

120 Sodium dodecyl sulfate-polyacrylamide gel electrophoresis (SDS-PAGE) was used to determine the
121 protein profiles of the germinated chickpea isolates and GCPH. A previously established protocol was
122 followed to analyze proteins with molecular weights of 10 - 250 kDa[23].

123 *2.5 Identification and characterization of peptides from GCPH*

124 An established peptide sequencing procedure was used [25]. Peptides in the hydrolysate were identified
125 using liquid chromatography-electrospray ionization-mass spectrometry/mass spectrometry (LC-ESI-
126 MS/MS). MassLynx V4.1 (Waters Corporation, Milford, MA, USA) was used to determine the peptides.
127 Peptides were identified using MS peaks, and those that were reproducible in independent replicates with
128 a probability of >50% were used for further analysis.

129 The source of the peptides and their physiochemical, bioactive, and bitter properties were analyzed
130 using the BLAST [26], PepDraw[27] and BioPep [28] databases. ToxinPred was used to predict the toxicity of
131 the peptides[29]

132 *2.6 Molecular docking of peptides identified in GCPH*

133 Prior to molecular docking, crystallographic structures were prepared by removing water molecules,
134 removing ligands and unbound molecules using Discovery Studio v4.1 (Waltham, MA, USA). Peptides
135 identified in storage proteins were analyzed using molecular docking, performed with Autodock Vina
136 v1.5.6 (La Jolla, CA, USA) [30]. Peptide structures were drawn using MarvinSketch (ChemAxon, Boston,
137 MA, USA). The crystallographic structures of DPP-IV (PDB ID: 6B1E), SGLT1 (PDB ID: 2XQ2), the
138 N-terminal of sucrase-isomaltase (PDB ID: 3PLL) were obtained from the RCSB protein data bank. The
139 crystal structure for T2R4 and T2R14 was obtained from BitterDB [31]. The crystal structure for GLUT2
140 was obtained using a previously established protocol [30]. Molecular docking sites were determined using
141 previously identified active sites of the respective markers [32–40].Visualizations were prepared to identify
142 docking patterns, specifically the different types of interactions and the strongest contributors to
143 inhibition or activation of the specific marker. The energy of affinity with the active site was determined
144 and visualized using Discovery Studio v4.1 (Waltham, MA, USA).

145 *2.7. DPP-IV and α-glucosidase inhibition*

146 DPP-IV inhibition was determined using the DPP-IV-Glo Kit (Promega, Madison, WI, USA) with the
147 manufacturer's protocol. α-Glucosidase inhibition was determined following a previously established

148 protocol [10]. Sitagliptin (100 μM) and acarbose (2 mM) was used as the positive control for DPP-IV and
149 α-glucosidase inhibition respectively.

150 *2.8. Evaluation of GCPH using Caco-2 cells in vitro*

151 Caco-2 cells were sub-cultured and maintained using a previously established protocol [30]. Caco-2
152 cells were subcultured for 16 to 21 days to achieve the morphology of intestinal epithelial cells. Viability
153 of cells with all treatments was measured using the CellTiter® 96 Aqueous One Solution Proliferation
154 assay (Promega, Madison, WI, USA) according to the manufacturer's protocol.

155 *2.8.1 Glucose uptake and sucrase-maltase-isomaltase activity*

156 A previously established protocol was followed [37] with few modifications. Briefly, Caco-2 cells were
157 seeded in 96-well plates at 5×10^4 cells/well for 16 to 21 days. Cells were treated with GCPH at
158 concentrations 100 μM, 250 μM, 500 μM, 1000 μM and 2500 μM. Pure peptides FDLPAL, GEAGR and
159 VVFW were tested at concentrations of 50 μM, 100 μM and 250 μM. Phloretin (PHL, 100 μM) was used
160 as a positive control.

161 For SI activity, a previously established protocol was followed with changes[17]. Cells were plated
162 similar to the glucose uptake assay and were treated with GCPH or pure peptides for 24 h at the same
163 concentrations as done with the glucose uptake assay. Following this, media was changed to contain
164 either 20 mM of sucrose, maltose or isomaltose, along with different concentrations of GCPH and pure
165 peptides tested. The media were collected, and the glucose levels were measured using the Amplex Red
166 Glucose/Glucose Oxidase Kit from Thermo Fisher. Acarbose (2 mM) was used as the positive control.

167 *2.8.2 DPP-IV inhibition*

168 DPP-IV inhibition in the upper cell media was determined in Caco-2 cells using the DPP-IV-Glo Kit
169 (Promega, Madison, WI, USA) according to the manufacturer's protocol. Sitagliptin (500 μM) was used
170 as the positive control.

171 *2.9 Western blot analysis*

172 Protein expression of GLUT2, SGLT1, T2R4, T2R14, PLCβ2, TRPM5 and β-actin were analyzed in
173 Caco-2 cells A previously established protocol was followed with slight modification [37]. Cells were
174 cultured as indicated in 2.8.1 and stimulated with 30 mM glucose. The protein concentration of the
175 sample loaded was changed with increasing concentration of hydrolysate treatment to account for protein
176 absorbed during treatment (20 μg for the untreated sample, positive controls, cells treated with 100 μM
177 and 250 μM of GCPH and all concentrations of pure peptides, 25 μg for the 500 μM sample, 40 μg for
178 the 1000 μM and 60 μg for the 2500 μM sample). The following reagents were used as positive controls
179 for bitter taste receptor activation at a concentration of 100 μM: flufenamic acid (FA) for the activation of
180 T2R14, phloretin (PHL) for the activation of PLCβ2, denatonium benzoate (DB) for the activation of
181 T2R4 and TRPM5. Western blot bands were quantified using ImageJ (NIH, USA), using the measure
182 tool. The intensity of bands from each marker was normalized to β-actin.

183 *2.10 Statistical analysis*

184 All the experimental procedures were performed in duplicate or triplicate to ensure reproducibility.
185 Data are presented as mean ± standard deviation. Statistical analysis was performed using one-way
186 ANOVA unless specified otherwise. A p-value of < 0.05 was considered as statistically significant. A
187 correlation plot was constructed using R to integrate the information presented.

188 **3. Results and Discussion**

189 *3.1 Hydrolysis and sodium dodecyl sulfate-polyacrylamide gel electrophoresis of germinated*
190 *chickpea protein*

191 The intensity of protein bands above 100 kDa was significantly lower in germinated chickpeas than in
192 non-germinated chickpea protein isolates, as seen in **Figure 1A** and **Figure 1B**. The action of
193 endoproteases during germination allows the seed to use the protein for growth, resulting in lower
194 molecular masses with increasing germination time [3]. The protein profile obtained using SDS-PAGE is
195 shown in **Figure 1C**. The intensities of the bands at different molecular masses were analyzed and are
196 summarized in **Figure 1D**. The intensity of proteins with molecular masses of 18–101 kDa was

197 significantly different between the germinated protein isolate and the hydrolyzed germinated protein
198 isolate. These proteins were not present in the germinated chickpea protein isolate, indicating that they are
199 formed during hydrolysis. Using principal component analysis, germination time was found to play a
200 significant role in increasing the anti-diabetic potential of chickpea protein hydrolysate produced with
201 ficin based on DPP-IV inhibition [23]. Among the germination times evaluated (2-day, 4-day, and 6-day), 6-
202 day germination produced a hydrolysate with the highest anti-diabetic activity [23]. Ficin has narrow
203 specificity, resulting in hydrolysates with molecular masses of <30 kDa. Black bean and mung bean
204 proteins hydrolyzed with ficin resulted in proteins with molecular masses of 10–30 kDa [41], which is
205 similar to the results found in our study. Thus, the specificity of ficin with regard to legume proteins was
206 confirmed.

207 *3.2 Peptide identification and characterization by LC-ESI-MS/MS*

208 Forty peaks above 30% of the height of the tallest peak were identified. A total of 32 peptides were
209 reproducible with a probability of over 50%. Three peptides were identified to be from storage proteins:
210 VVFW (Val-Val-Phe-Trp), FDLPAL (Phe-Asp-Leu-Pro-Ala-Leu), and GEAGR (Gly-Glu-Ala-Gly-Arg)
211 from legumin. The physiochemical, bioactive and bitterness properties of these peptides is outlined in
212 **Table 1**. Additionally, the hydrophobicity of peptides tested in molecular docking and *in vitro* assays is
213 outlined in **Table 1**. In biochemical and *in vitro* assays, pure peptides were dissolved in water or media.
214 Peptide FDLPAL and GEAGR readily dissolved, whereas a non-toxic amount of DMSO with peptide
215 VVFW was used. All three peptides used in molecular docking, namely FDLPAL, VVFW and GEAGR
216 were predicted to be non-toxic on ToxinPred.

217 The peptide sequencing process is outlined in **Supplementary Figures 1A and 1B.** Peptides from
218 metabolic sources are outlined in **Supplementary Table 1**. Molecular masses of the peptides ranged from
219 364.16–1192.62 g/mol. The average molecular mass was estimated as 640 g/mol. Notably, all peptides
220 contained fragments with DPP-IV inhibitory properties and all peptides, excluding STSA, presented bitter
221 fragments.

222 Hydrolysates produced using raw chickpea proteins and a simulated GI system showed molecular
223 masses of 363.2–1806.4 g/mol [9]. Peptides from other germinated protein hydrolysates produced using a
224 simulated GI system showed molecular masses ranging from 788.4–1388.7 g/mol [42] and 574.32–1448.81
225 g/mol [43] in soybean and common bean respectively. This indicated that the relatively broader specificity
226 of ficin, in comparison to pepsin and pancreatin, contributed to the lower molecular masses of the
227 peptides.

228 Peptides VVFW and FDLPAL were previously identified in hydrolysates produced with precooked
229 chickpea proteins and bromelain [10]; in addition, a peptide similar to SPGAGKG was found in precooked
230 and cooked chickpea protein hydrolysates. Peptides found in the *in silico* hydrolysis of chickpea legumin
231 with ficin [44] did not match the peptides found in this study most likely due to changes in the proteins
232 during germination.

233 *3.3 DPP-IV, α-glucosidase and sucrase-isomaltase inhibition*

234 **Table 2** presents the results of the molecular docking of peptides with different markers related to
235 glucose and lipid metabolism.

236 Peptide FDLPAL in molecular docking with DPP-IV is shown in **Figure 2A** and its position in
237 interacting with DPP-IV is shown in **Figure 2B**. Peptide VVFW in molecular docking with DPP-IV is
238 shown **Figure 2C** and its position in interacting with DPP-IV is shown in **Figure 2D**. Molecular docking
239 of GEAGR with DPP-IV is shown in **Figure 2E** and the position of the peptide in the interaction with
240 DPP-IV is shown in **Figure 2F**. The peptide GEAGR had the highest energy of affinity to DPP-IV at -8.3
241 kcal/mol. Previously, the energy of affinity documented for peptide FDLPAL was -5.7 kcal/mol, whereas
242 it was -8.2 kcal/mol in this study [10]. Similarly, in the case of peptide VVFW, a previous study identified
243 the energy of affinity at -3.2 kcal/mol, whereas it was -7.4 kcal/mol in this study. The difference in
244 energies is likely due to the variations in the arrangement during the docking process and docking
245 position of the peptide, which is also evident from the peptide fragments associated with docking. The

246 difference is also reflected in the energy of affinity in the positive control (vildagliptin), which is much
247 higher than that previously documented (-7.5 kcal/mol).

248 GCPH showed an IC_{50} of 370 μM (0.2 mg/mL) for the biochemical inhibition of DPP-IV (**Figure**
249 **2G**). In comparison, peptides FDLPAL, VVFW, and GEAGR showed a maximum DPP-IV inhibition of
250 11.4, 11.1 %, and 9.7%, respectively, at 250 μM. In Caco-2 cells, GCPH showed an IC_{50} of 2100 μM for
251 DPP-IV inhibition (**Figure 2H**). In comparison, pure peptides did not show significant DPP-IV inhibition
252 compared with non-treated cells (**Table 3**).

253 The active site of DPP-IV has been shown to contain residues Ser630, Tyr666, Tyr547, Trp629 and
254 Asn710 [33], all of which were found in the molecular docking interactions presented in this study.
255 Although peptide GEAGR had the strongest energy of affinity with DPP-IV, residues Arg125 and
256 Tyr547, which had the shortest distances in interactions with the peptide (**Table 2**), these residues shown
257 to have unfavorable interactions with the peptide. As seen with biochemical and *in vitro* assays (**Table 3**),
258 this unfavorable interaction may have contributed to the limited DPP-IV inhibition seen with pure
259 peptides. Similarly with peptides FDLPAL and VVFW, unfavorable interactions were again seen with
260 Arg125 along with a short distance between the protein and the ligand.

261 Raw chickpea protein hydrolysate produced using a simulated GI system showed higher (less active)
262 IC_{50} values for DPP-IV inhibition (0.3 mg/mL) [45]. Chickpea protein hydrolysates produced with
263 bromelain showed a comparable IC_{50} (0.2 mg/mL) in the inhibition of DPP-IV [10]. A mixture of three
264 peptides (FEI, FEL, and FIE) presented an IC_{50} of 4.2 μg/mL for DPP-IV inhibition [46]

265 Two peptides identified in GCPH, SPGAGKG and GLAR, had an IC_{50} values of 0.27 mg/mL and
266 12.7 mg/mL, respectively, in DPP-IV inhibition [23].

267 DPP-IV is a peptidase that prefers alanine and proline residues at the P2 position. However, substrates
268 with other residues such as valine and glycine are also cleaved by DPP-IV, thereby rendering the peptide
269 ineffective in binding with DPP-IV [47]. We have shown that pure peptides are less potent than whole
270 hydrolysates, which is likely due to the proteolytic action of DPP-IV. DPP-IV contains three regions, the

271 S1, S2 and N-terminus regions, of which the S1 and N-terminus regions are crucial in determining its
272 activity. The S1 region is primarily composed of hydrophobic amino acids, whereas the N-terminus
273 contains hydrophilic residues[32]. A mixture of peptides is therefore more favorable than pure peptides in
274 effectively inhibiting the action of DPP-IV, as more peptides are available to bind to the active sites of
275 DPP-IV.

276 To the best of our knowledge, GCPH produced with ficin has not been tested for its DPP-IV
277 inhibition potential *in vitro.* Two peptides identified from lupin (LTFPGSAED) and soybean
278 (IAVPTGVA) were evaluated for their DPP-IV inhibitory activity in Caco-2 cells, wherein an IC_{50} of 228
279 and 106 μM, respectively, was found [48]. Oat globulins presented an IC_{50} of 188.1 μg/mL for the inhibition
280 of DPP-IV [49]. In previous studies, DPP-IV inhibition was evaluated in Caco-2 cells in the absence of
281 glucose stimulation. DPP-IV activity has been positively correlated with hyperglycemia, which may
282 result in the need for a higher concentration of hydrolysate to effectively inhibit DPP-IV [50].

283 In the molecular docking studies with SI, peptide FDLPAL showed the highest energy of affinity of (-
284 7.3 kcal/mol). The positive control (kotalanol) had an affinity energy of -6.1 kcal/mol. Molecular docking
285 of FDLPAL with SI is outlined in **Figure 3A** and the position of the peptide in the interaction with SI is
286 shown in **Figure 3B**. The molecular docking of peptides VVFW and its position with SI is outlined in
287 **Figures 3C and 3D,** respectively, and the same for peptide GEAGR in the interaction with SI is shown in
288 **Figures 3E and 3F, respectively**.

289 GCPHs showed an IC_{50} of 190 μM (0.1 mg/mL) in the biochemical inhibition of α-glucosidase
290 (**Figure 3G**). Peptide VVFW showed α-glucosidase inhibition of 20% at 250 μM. α-Glucosidase
291 inhibition was not seen in peptides FDLPAL and GEAGR.

292 α-Glucosidases consist of enzymes that hydrolyze starches to monosaccharides. In Caco-2 cells, α-
293 glucosidase activity is associated with SI, which hydrolyzes sucrose, maltose and isomaltose into glucose
294 for absorption [35]. GCPH presented a bell-shaped curve in the inhibition of sucrase (**Figure 3H**), maltase
295 and isomaltase (**Table 3**). At 500 μM (0.32 mg/mL), the hydrolysate was most effective at inhibiting

296 sucrase (58.5%) and isomaltase (64.8%) at 500 μM. At 1000 μM, the hydrolysate was most potent in
297 inhibiting maltase (46.3%).

298 Among peptides tested, FDLPAL showed the highest inhibition of sucrase activity (44.1%) at 100 μM
299 **(Table 3).**

300 Maltase activity inhibition was the highest with 50 μM FDLPAL (63.4%) and GEAGR (59.6%).
301 There was no significant difference between the maltase activity of cells treated with 50 μM and 100 μM
302 of the pure peptides FDLPAL and GEAGR, respectively.

303 Isomaltase inhibition was the highest with 50 μM FDLPAL (51.9%) and GEAGR (46.4%). The
304 positive control, acarbose (2 mM), presented sucrase, maltase, and isomaltase inhibition values of 25.7%,
305 74.8%, and 39.1%, respectively. No differences in cell viability were seen in cells stimulated with
306 sucrose, maltose or isomaltose (**Supplementary Figure 2A and 2B**).

307 FDLPAL presented the highest energy of affinity (-7.3 kcal/mol) in molecular docking with SI and
308 was bound to previously known residues that are part of the active site of SI (Asp571 and Lys509) [35].
309 Specifically, these residues were bound through hydrogen bonds and there were no unfavorable
310 interactions. This is reflected in the *in vitro* assay, wherein FDLPAL had the highest inhibition of sucrase,
311 maltase and isomaltase at 100 μM. Peptide GEAGR also showed high SI inhibition, despite having a
312 lower energy of affinity with SI in molecular docking. In molecular docking with SI, GEAGR showed
313 hydrogen bonding with residues Arg555 and Lys509 with shorter bonds compared to the unfavorable
314 interaction. Additionally, all residues were bound through hydrogen bonding which may contribute to its
315 SI inhibitory activity. Compared to peptides FDLPAL and GEAGR, peptide VVFW primarily contained
316 van der Waals interactions, which are weaker in comparison to hydrogen bonding. Additionally, the
317 residues bound to peptide VVFW are not known to be associated with SI's active site, in line with the SI
318 inhibition results presented in this study.

319 Both GCPH and pure peptides presented bell-shaped inhibition of SI with increasing concentrations.
320 SI is an essential enzyme for the digestion and absorption of carbohydrates. SI deficiency is associated

321 with malnutrition and digestive problems [34]. Therefore, higher concentrations of pure peptides may be too
322 potent in the inhibition of SI, leading to a feedback response that increases SI production to reduce
323 detrimental effects.

324 To the best of our knowledge, protein hydrolysates have not yet been tested for their effects on SI
325 activity. Other food-derived compounds were studied for their effect on SI activity, such as the flavonoid
326 melanoxetin (IC_{50} 2.2 μM and 2.5 μM for sucrase and isomaltase activity, respectively) [51]. Tea extracts
327 from black tea showed IC_{50} values of 8.3 μg/mL, 16.1 μg/mL, and 21.6 μg/mL in sucrase, maltase, and
328 isomaltase inhibition, respectively [17].

329 *3.4 Glucose uptake, SGLT1 and GLUT2 expression in Caco-2 cells*

330 The molecular docking of FDLPAL and its position with SGLT1 is outlined in **Figures 4A and 4B,**
331 respectively. In molecular docking with SGLT1, peptide VVFW showed the highest energy of affinity of
332 (-9.9 kcal/mol). The positive control (phlorizin) had an affinity of -9.1 kcal/mol. Molecular docking of
333 VVFW with SGLT1 is shown in **Figure 4C** and the position of the peptide is outlined in **Figure 4D.** The
334 molecular docking of GEAGR and its position with SGLT1 is outlined in **Figures 4E and 4F,**
335 respectively. Most ligand-protein interactions for peptides FDLPAL and VVFW are van der Waal's
336 interactions, as seen in **Figure 5**. Hydrogen bonding was present with peptide GEAGR and SGLT1 in
337 molecular docking; however, only four residues participate in this interaction and with an energy of
338 affinity of -6.9 kcal/mol. Importantly, all three peptides do not interact with residues that have previously
339 been associated with the 'activation' of SGLT1, namely Tyr290, Thr287 and His83, which likely affects
340 the peptides' ability to regulate SGLT1 expression [36].

341 Regarding GLUT2, the molecular docking of FDLPAL is outlined in **Figures 5A** and the position of
342 the peptide in its interaction with GLUT2 is outlined in **Figures 5B**. Peptide VVFW showed the highest
343 energy of affinity (-10.0 kcal/mol) with GLUT2. The positive control (phloretin) had an energy of affinity
344 of -9.1 kcal/mol. Molecular docking of VVFW is shown in **Figure 5C** and the position of the peptide is

345 shown in **Figure 5D**. The molecular docking of GEAGR with GLUT2 is outlined in **Figures 5E** and the
346 position of the peptide in its interaction with GLUT2 is outlined in **Figures 5F**.
347 In molecular docking with GLUT2, peptide VVFW, which had the strongest energy of affinity (-10.0
348 kcal/mol), showed hydrogen bonding with residues Asn347, Gln312, Ile28 and Gln313. Additionally,
349 His309 showed Pi-Pi interactions with the phenylamine residue present in peptide VVFW. Previously,
350 these four residues have been shown to contribute to inhibition of glucose uptake through GLUT2 [37].
351 Regarding peptide FDLPAL, hydrogen bonding was seen with residues Gln313 and His309, in addition to
352 van der Waals interactions involving residues Ile28 and Phe102, which were previously identified to
353 contribute to the inhibition of GLUT2. However, an unfavorable interaction with Gln312 reduced the
354 overall energy of affinity. Finally with peptide GEAGR, despite all interactions between hydrogen
355 bonding, only three residues, namely His309, Ser167 and Trp442 have been shown to contribute to
356 GLUT2 inhibition.
357 A dose-dependent response inhibiting glucose uptake was observed in Caco-2 cells treated with
358 GCPH (IC_{25} 2.07 mM or 1.3 mg/mL) (**Figure 6A**). No significant difference was observed in cell
359 viability (**Supplementary Figure 2C and 2D**) ($p > 0.05$). Peptide VVFW was the most potent inhibitor
360 of glucose uptake with a 38.7% inhibition at 50 μM (**Figure 6B**). Inhibition of glucose uptake was lower
361 at 250 μM than at 50 μM. To maintain glucose uptake at healthy levels, cells may respond to potent
362 inhibitors by increasing glucose uptake. The glucose uptake of peptide VVFW is in line with the
363 molecular docking results, as it had the highest energy of affinity with SGLT1 and GLUT2 and
364 correspondingly, the lowest glucose uptake among the peptides tested.
365 Previously, pure peptides and a protein fraction from black bean protein were evaluated for their
366 effects on glucose uptake in Caco-2 cells [37]. Glucose uptake was significantly inhibited by 100 μM of
367 each peptide. The protein fraction inhibited glucose uptake by approximately 30% at a concentration of
368 10 mg/mL.

369 SGLT1 expression was not significantly different from that in untreated cells when treated with
370 GCPH or pure peptides as seen in **Figure 6C** and **Figure 6D** respectively. GLUT2 expression was
371 significantly reduced at GCPH concentrations of 500, 1000, and 2500 μM (**Figure 6E**). GLUT2
372 expression was significantly lower with all peptides compared to the untreated control (**Figure 6F**).
373 The results obtained with GLUT2 molecular docking are in line with glucose uptake and GLUT2
374 western blot results. Namely, peptide VVFW had the strongest energy of affinity with GLUT2 and
375 interacted with known residues associated with GLUT2 inhibition. As seen in **Figure 6B** and **Figure 6F**,
376 peptide VVFW resulted in the lowest glucose uptake and lowered GLUT2 expression significantly
377 compared to non-treated cells.
378 With peptides FDLPAL and GEAGR, the energy of affinity with GLUT2 was lower, but known
379 residues that result in the inhibition of GLUT2 were present, resulting in lowered expression of GLUT2
380 seen in western blot results and lower glucose uptake than the non-treated control. However, compared to
381 peptide VVFW, peptides FDLPAL and GEAGR were relatively less potent in reducing glucose uptake,
382 which is in line with molecular docking results.
383 *3.5 Expression of bitter taste receptors T2R4 and T2R14 and associated markers of the signaling*
384 *pathway in Caco-2 cells*
385 The molecular docking of peptides FDLPAL with T2R4 and its position is shown in **Figures 7A and**
386 **7B,** respectively, and the same for peptide VVFW is shown in **Figures 7C and 7D**, respectively.
387 In molecular docking studies with T2R4, peptide GEAGR showed the highest energy of affinity (-5.9
388 kcal/mol). The positive control (denatonium benzoate, DB) had an affinity energy of -6.6 kcal/mol. The
389 molecular docking energy of the peptide GEAGR with T2R4 is shown in **Figure 7E**, and its position is
390 shown in **Figure 7F.**
391 A previous study showed that known activators of T2R4 bind to amino acid residues Tyr250 and
392 Leu181 [38]. Peptide VVFW presents van der Waals interactions with Tyr250 and Leu181, whereas peptide
393 GEAGR does not have interactions with any known residues associated with activation of T2R4.

394 Although peptide GEAGR showed the strongest energy of affinity as a result of hydrogen bonding, the
395 residues itself are not associated with the activation or blocking of T2R4.
396 Conversely with peptide FDLPAL, van der Waals interactions are primarily present, leading to a
397 lower energy of affinity. Although interactions with Tyr250 and Leu181 are present in this case, the
398 distance with Leu181 is longer compared to peptide VVFW and the interaction with Tyr250 is a Pi-Alkyl
399 interaction, as compared to a Pi-Pi interaction with peptide VVFW, which is stronger. The molecular
400 docking results are in line with the results presented in the western blot, wherein peptide VVFW
401 increased the expression of T2R4.
402 The molecular docking of peptides FDLPAL with T2R14 and its position is shown in **Figures 8A and**
403 **8B** respectively. In molecular docking studies with T2R14, peptide VVFW showed the highest energy of
404 affinity (-10.5 kcal/mol). The positive control, flufenamic acid, had an affinity of -5.9 kcal/mol.
405 Molecular docking of VVFW with T2R14 is shown in **Figure 8C** and its position with T2R14 is shown in
406 **Figure 8D.** The molecular docking of peptide GEAGR with T2R14 is shown in **Figures 8E and 8F,**
407 respectively. Residues of molecular docking with bitter taste receptors 4 and 14 is summarized in
408 **Supplementary Table 2.**
409 In Caco-2 cells treated with GCPH, expression of the bitter taste receptor T2R4 was significantly
410 reduced in a dose-dependent manner (**Figure 9A**), whereas T2R14 expression increased significantly in a
411 dose-dependent manner (**Figure 9B**). PLCβ2 expression was significantly lower in Caco-2 cells treated
412 with 500 μM, 1000 μM, and 2500 μM GCPH (**Figure 9C**). TRPM5 expression was significantly higher
413 in Caco-2 cells treated with 250 μM hydrolysate (**Figure 9D**). At concentrations of 500, 1000, and 2500
414 μM, TRPM5 expression was significantly lowered. Piperine has previously shown to activate T2R14 and
415 further release GLP-1 in a different line of Caco-2 cells [52]. Consistent with this study, GCPH was more
416 potent in inhibiting DPP-IV, which would in turn increase GLP-1 production.
417 The expression of the bitter receptor T2R4 increased significantly in a dose-dependent manner when
418 Caco-2 cells were treated with peptide VVFW. The other peptides showed no differences in T2R4

419 expression **(Figure 9E**). When treated with pure peptides, T2R14 expression was significantly reduced
420 when treated with peptides GEAGR (250 μM) and VVFW (50 and 100 μM) **(Figure 9F).**
421 A previous study showed that the amino acid residues His94 and Gln266 played important roles in the
422 activation of T2R14 [39]. In molecular docking, these residues (His94 and Gln266) were not involved in the
423 interaction with the peptides identified in this study. Flufenamic acid interacted with Gln266, which may
424 have resulted in the activation of T2R14, as this residue has previously been associated with the activation
425 of T2R14.
426 Peptide VVFW had the highest energy of affinity and also reduced the expression of T2R14
427 significantly compared to the non-treated control, as seen in **Figure 9F**. Peptide VVFW presented van der
428 Waals interactions with residues Trp89 and Ile262, and hydrogen bonding with Asn157, which have all
429 previously been shown to be involved in the blocking of T2R14 [38-39]. Peptide GEAGR, which also
430 reduced expression of T2R14 at 250 μM, showed hydrogen bonding with Thr86 and Asn157, and Pi-Pi
431 interactions with Trp89, which have been associated with blocking T2R14, as seen at 250 μM in western
432 blots (**Figure 9F**) [38-39]. Future studies may focus on further understanding which of the residues
433 contribute more to the blocking of T2R14.
434 Regarding PLCβ2 expression with pure peptides, FDLPAL and GEAGR showed lowered expression
435 at all concentrations tested, whereas VVFW lowered expression only at 50 μM compared to non-treated
436 cells (**Figure 9G**). TRPM5 expression was lowered by all peptides and the expression was lowest with
437 peptide VVFW at 50 μM (**Figure 9H**). At the same concentration, glucose uptake was the lowest among
438 the samples tested.
439 A negative correlation was also observed between the expression of T2R4 and T2R14 in Caco-2 cells
440 (R value = -0.67) (**Table 4**). T2R14 is activated by a broader range of substrates than T2R4 [40]. However,
441 the peptides identified in this study were able to bind to the epitope of T2R14 and residues that contribute
442 to the blocking of T2R14. This likely contributed to the reduced expression of T2R14 by peptides
443 GEAGR at 250 μM and VVFW at 50 μM and 100 μM.

444 In sweet, bitter and umami taste signaling, the βγ subunits dissociate from the G-protein complex
445 when an agonist binds to the active site of the bitter taste receptor, which in turn activates PLCβ2. Upon
446 activation, PLCβ2 activates the release of calcium from 1,4,5-inositol triphosphate (IP3) dependent stores,
447 which opens TRPM5 channels [21].

448 A strong positive correlation was observed between PLCβ2 and GLUT2 (R value = 0.77) as well as
449 between GLUT2 and TRPM5 expression (R value = 0.80) (**Table 4**). Previously, inhibition of PLCβ2 has
450 been found to reduce calcium influx in Caco-2 cells through CaV1.3 and consequently reduced GLUT2
451 translocation from the basolateral to the apical side [53]. In sweet, bitter and umami taste signaling, reduced
452 PLCβ2 may lead to a reduced release of intracellular calcium stores, which in turn reduces TRPM5
453 expression, GLUT2 expression, and glucose uptake.

454 Overall markers PLCβ2 and TRPM5, which are shared by the sweet, bitter and umami taste signaling
455 pathways, were blocked by GCPH at concentrations of 500 μM or higher and by all concentrations of all
456 peptides tested. The same samples reduced GLUT2 expression as well. Thus, blocked taste signaling
457 associated with G-Protein coupled receptor activation may be favorable in reducing glucose uptake.
458 Previously, bitter signaling has been shown to interact and suppress sweet taste signaling [54]. Further
459 investigation into the interactions between bitter and sweet signaling is needed to understand the role of
460 bitterness in glucose uptake by Caco-2 signaling.

461 In summary, the results suggest on the apical side, both GCPH and pure peptides inhibited SI activity,
462 thereby reducing the total amount of glucose available for absorption. Further, GCPH and pure peptides
463 reduced GLUT2 expression. The reduced expression of GLUT2 and overall reduction in glucose uptake
464 by Caco-2 cells also contributed to reduced PLCβ2 and TRPM5 expression. This, in turn, will likely
465 reduce calcium influx within the cell, thereby preventing GLUT2 translocation from the basolateral side
466 to the apical side. Additionally, GCPH also inhibited DPP-IV activity. Further investigation on the
467 interactions between bitter and sweet receptors, and their subsequent effect on PLCβ2 and TRPM5 is

468 needed to understand the role of bitter receptors in this mechanism. A proposed mechanism is outlined in

469 **Supplementary Figure 3**.

470 *4. Conclusion*

471 Germinated chickpea protein hydrolysate was found to significantly inhibit DPP-IV and α-
472 glucosidase in biochemical assays. In molecular docking, peptides identified in the GCPH showed strong
473 interactions with residues associated with the inhibition of SI, GLUT2 and T2R14, which was reflected in
474 *in vitro* assays. In Caco-2 cells, dose-dependent inhibition of glucose uptake and concurrent inhibition of
475 the bitter receptor signaling pathway were observed. Chickpea protein hydrolysate produced using 6-day
476 germinated chickpea and ficin has the potential to be incorporated into commercial foods as a functional
477 ingredient. Germinated chickpea protein hydrolysates may be used as a functional ingredient in
478 commercial foods such as baking mixes for cakes, brownies, muffins and pancakes, tortillas, to increase
479 bioactive properties of the food, protein content and act as an emulsifier.

480

481 **CRediT authorship contribution statement**

482 Subhiksha Chandrasekaran: Data curation, Formal analysis, Investigation, Methodology, Software,
483 Validation, Visualization, Writing - original draft. Elvira de Mejia: Conceptualization, Funding
484 acquisition, Methodology, Project administration, Resources, Supervision, Visualization, Writing -
485 review & editing.

486 **Declaration of Competing Interest**

487 The authors declare that they have no known competing financial interests or personal relationships
488 that could have appeared to influence the work reported in this paper.

489 **Acknowledgements**

490 Research was supported by the USDA Pulse Crop Health Initiative's funding 58-3060-9-045.
491 Chickpea varieties were provided by Dr. George J. Vandemark from the USDA. The authors thank Lily
492 Lincoln and Carolyn Liu for their help with experiments.

493 **References**

494 1 *Food & Agriculture Organization of the United Nations, https://www.fao.org/faostat/en/#home,*
495 *(accessed March 2023)*
496 2 R. Tso, A. J. Lim and C. G. Forde, Unintended Consequences: Nutritional Impact and Potential
497 Pitfalls of Switching from Animal-to Plant-Based Foods, *Foods,* 2021, **10**, 24.
498 3 I. C. Ohanenye, A. Tsopmo, C. E. C. C. Ejike and C. C. Udenigwe, Germination as a bioprocess
499 for enhancing the quality and nutritional prospects of legume proteins, *Trends Food Sci. Technol.*,
500 2020, **101**, 213-222.
501 4 S. Harini, K. Adilaxmamma, E. M. Mohan, C. Srilatha and M. A. Raj, Antihyperlipidemic activity
502 of chickpea sprouts supplementation in ovariectomy-induced dyslipidemia in rats, *J. Ayurveda*
503 *Integr. Med.*, 2015, **6**, 104.
504 5 R. K. Mamilla and V. K. Mishra, Effect of germination on antioxidant and ACE inhibitory
505 activities of legumes, *LWT - Food Sci. Technol.*, 2017, **75**, 51-58.
506 6 E. Di Stefano, A. Tsopmo, T. Oliviero, V. Fogliano and C. C. Udenigwe, Bioprocessing of
507 common pulses changed seed microstructures, and improved dipeptidyl peptidase-IV and α-
508 glucosidase inhibitory activities, *Sci. Reports*, 2019, **9**, 1–13.
509 7 H. Korhonen and A. Pihlanto, Bioactive peptides: Production and functionality, *Int. Dairy J.*, 2006,
510 **16**, 945–960.
511 8 C. Moreno, L. Mojica, E. González De Mejía, R. María, C. Ruiz and D. A. Luna-Vital,
512 Combinations of legume protein hydrolysates synergistically inhibit biological markers associated
513 with adipogenesis, *Foods,* 2020, **9**, 1678.
514 9 C. Torres-Fuentes, M. D. M. Contreras, I. Recio, M. Alaiz and J. Vioque, Identification and
515 characterization of antioxidant peptides from chickpea protein hydrolysates, *Food Chem.*, ,2015,
516 **180**, 194-202.
517 10 K. A. Acevedo Martínez and E. Gonzalezde Mejia, Comparison of five chickpea varieties,

518 optimization of hydrolysates production and evaluation of biomarkers for type 2 diabetes, *Food*
519 *Res. Int.*, 2021, **147**, 110572.
520 11 X. Xu, Y. Qiao, B. Shi and V. P. Dia, Alcalase and bromelain hydrolysis affected physiochemical
521 and functional properties and biological activities of legume proteins, *Food Struct.*, 2021, **27**,
522 100178
523 12 S. Chatterjee, K. Khunti and M. J. Davies, Type 2 diabetes, *Lancet*, 2017, **38**, 2239-2251.
524 13 K. A. Acevedo Martinez, M. M. Yang and E. Gonzalez de Mejia, Technological properties of
525 chickpea (*Cicer arietinum)*: Production of snacks and health benefits related to type-2 diabetes,
526 *Compr. Rev. Food Sci. Food Saf.*, 2021, **20**, 3762–3787.
527 14 C. P. Kulkarni, J. M. Thevelein and W. Luyten, Characterization of SGLT1-mediated glucose
528 transport in Caco-2 cell monolayers, and absence of its regulation by sugar or epinephrine, *Eur. J.*
529 *Pharmacol.*, 2021, **897**, 173925.
530 15 Y. Zheng, J. S. Scow, J. A. Duenes and M. G. Sarr, Mechanisms of glucose uptake in intestinal cell
531 lines: role of GLUT2, *Surgery*, 2012, **151**, 13–25.
532 16 J. Caron, D. Domenger, P. Dhulster, R. Ravallec and B. Cudennec, Using Caco-2 cells as novel
533 identification tool for food-derived DPP-IV inhibitors, *Food Res. Int.*, 2017, **92**, 113–118.
534 17 S. Liu, Z. Ai, Y. Meng, Y. Chen and D. Ni, Comparative studies on the physicochemical profile
535 and potential hypoglycemic activity of different tea extracts: Effect on sucrase-isomaltase activity
536 and glucose transport in Caco-2 cells, *Food Res. Int.*, 2021, **148**, 110604.
537 18 J. Jeruzal-Świątecka, W. Fendler and W. Pietruszewska, Clinical role of extraoral bitter taste
538 receptors, *Int. J. Mol. Sci.,* 2020, **21**, 5156.
539 19 Y. Yu, G. Hao, Q. Zhang, W. Hua, M. Wang, W. Zhou, S. Zong, M. Huang and X. Wen, Berberine
540 induces GLP-1 secretion through activation of bitter taste receptor pathways, *Biochem.*
541 *Pharmacol.*, 2015, **97**, 173–177.
542 20 Y. Xia, L. Zhu, G. Wu, T. Liu, X. Li, X. Wang and H. Zhang, Comparative study of various

543 methods used for bitterness reduction from pea *(Pisum sativum L.)* protein hydrolysates, *LWT*,
544 2022, **159**, 113228.
545 21 Y. Zhang, M. A. Hoon, J. Chandrashekar, K. L. Mueller, B. Cook, D. Wu, C. S. Zuker and N. J. P.
546 Ryba, Coding of sweet, bitter, and umami tastes: different receptor cells sharing similar signaling
547 pathways, *Cell*, 2003, **112**, 293–301.
548 22 B. Liu, N. Li, F. Chen, J. Zhang, X. Sun, L. Xu and F. Fang, Review on the release mechanism and
549 debittering technology of bitter peptides from protein hydrolysates, *Compr. Rev. Food Sci. Food*
550 *Saf.*, 2022, **21**, 5153–5170.
551 23 S. Chandrasekaran and E. Gonzalez de Mejia, Optimization, identification, and comparison of
552 peptides from germinated chickpea *(Cicer arietinum)* protein hydrolysates using either papain or
553 ficin and their relationship with markers of type 2 diabetes, *Food Chem.*, 2022, **374**, 131717.
554 24 R. Morellon-Sterling, H. El-Siar, O. L. Tavano, Á. Berenguer-Murcia and R. Fernández-Lafuente,
555 Ficin: A protease extract with relevance in biotechnology and biocatalysis, *Int. J. Biol. Macromol.*,
556 2020, **162**, 394-404.
557 25 M. Grancieri, H. S. D. Martino and E. G. de Mejia, Protein digests and pure peptides from chia
558 seed prevented adipogenesis and inflammation by inhibiting PPARγ and NF-κB pathways in
559 3T3L-1 adipocytes, *Nutr.,* 2021, **13***,* 176.
560 26 E. W. Sayers, E. E. Bolton, J. R. Brister, K. Canese, J. Chan, D. C. Comeau, R. Connor, K. Funk,
561 C. Kelly, S. Kim, T. Madej, A. Marchler-Bauer, C. Lanczycki, S. Lathrop, Z. Lu, F. Thibaud-
562 Nissen, T. Murphy, L. Phan, Y. Skripchenko, T. Tse, J. Wang, R. Williams, B. W. Trawick, K. D.
563 Pruitt and S. T. Sherry, Database resources of the National Center for Biotechnology Information,
564 *Nucleic Acids Res.*, 2022, **50**, D20.
565 27 PepDraw, https://pepdraw.com/, (accessed 17th July 2022).
566 28 P. Minkiewicz, A. Iwaniak and M. Darewicz, BIOPEP_UWM Virtual - A Novel Database of
567 Food-Derived Peptides with In Silico-Predicted Biological Activity, *Appl. Sci. 2022, Vol. 12, Page*

568 *7204*, 2022, **12**, 7204.

569 29 S. Gupta, P. Kapoor, K. Chaudhary, A. Gautam, R. Kumar and G. P. S. Raghava, *In Silico*
570 Approach for Predicting Toxicity of Peptides and Proteins, *PLoS One*, 2013, **8**, e73957.

571 30 L. Mojica, E. Gonzalez de Mejia, M. Á. Granados-Silvestre and M. Menjivar, Evaluation of the
572 hypoglycemic potential of a black bean hydrolyzed protein isolate and its pure peptides using *in*
573 *silico, in vitro* and *in vivo* approaches, *J. Funct. Foods*, 2017, **31**, 274-286.

574 31 A. Dagan-Wiener, A. Di Pizio, I. Nissim, M. S. Bahia, N. Dubovski, E. Margulis and M. Y. Niv,
575 BitterDB: taste ligands and receptors database in 2019, *Nucleic Acids Res.*, 2019, **47**, D1179–
576 D1185.

577 32 J. P. Ambhore, P. S. Laddha, A. A. Kide, P. V. Ajmire, D. S. Chumbhale, A. B. Navghare, V. G.
578 Kuchake, P. J. Chaudhari and V. S. Adhao, Medicinal chemistry of non-peptidomimetic dipeptidyl
579 peptidase IV (DPP IV) inhibitors for treatment of Type-2 diabetes mellitus: Insights on recent
580 development, *J. Mol. Struct.*, 2023, 13524.

581 33 M. Nabeno, F. Akahoshi, H. Kishida, I. Miyaguchi, Y. Tanaka, S. Ishii and T. Kadowaki, A
582 comparative study of the binding modes of recently launched dipeptidyl peptidase IV inhibitors in
583 the active site, *Biochem. Biophys. Res. Commun.*, 2013, **434**, 191–196.

584 34 B. Gericke, M. Amiri and H. Y. Naim, The multiple roles of sucrase-isomaltase in the intestinal
585 physiology, *Mol. Cell. Pediatr. 2016 31*, 2016, **3**, 1–6.

586 35 L. Sim, C. Willemsma, S. Mohan, H. Y. Naim, B. M. Pinto and D. R. Rose, Structural basis for
587 substrate selectivity in human maltase-glucoamylase and sucrase-isomaltase N-terminal domains,
588 *J. Biol. Chem.*, 2010, **285**, 17763–17770.

589 36 E. Gorraitz, B. A. Hirayama, A. Paz, E. M. Wright and D. D. F. Loo, Active site voltage clamp
590 fluorometry of the sodium glucose cotransporter hSGLT1, *Proc. Natl. Acad. Sci. U. S. A.*, 2017,
591 **114**, E9980–E9988.

592 37 L. Mojica, D. A. Luna-Vital and E. Gonzalez de Mejia, Black bean peptides inhibit glucose uptake

593 in Caco-2 adenocarcinoma cells by blocking the expression and translocation pathway of glucose
594 transporters, *Toxicol. Reports*, 2018, **5**, 552-560.
595 38 M. Y. Yang, A. Mafi, S. K. Kim, W. A. Goddard and B. Guthrie, Predicted structure of fully
596 activated human bitter taste receptor TAS2R4 complexed with G protein and agonists, *QRB*
597 *Discov.*, 2021, **2**, E3.
598 39 R. Karaman, S. Nowak, A. Di Pizio, H. Kitaneh, A. Abu-Jaish, W. Meyerhof, M. Y. Niv and M.
599 Behrens, Probing the binding pocket of the broadly tuned human bitter taste receptor TAS2R14 bu
600 chemical modification of cognate agonists, *Chem. Biol. Drug Des.*, 2016, **88**, 66–75.
601 40 A. Di Pizio and M. Y. Niv, Promiscuity and selectivity of bitter molecules and their receptors,
602 *Bioorg. Med. Chem.*, 2015, **23**, 4082–4091.
603 41 Z. Zheng, J. Li, J. Li, H. Sun and Y. Liu, Physicochemical and antioxidative characteristics of
604 black bean hydrolysates obtained from different enzymes, *Food Hydrocolloids,* 2019, **97**, 105222.
605 42 M. González-Montoya, B. Hernández-Ledesma, J. M. Silván, R. Mora-Escobedo and C. Martínez-
606 Villaluenga, Peptides derived from in vitro gastrointestinal digestion of germinated soybean
607 proteins inhibit human colon cancer cells proliferation and inflammation, *Food Chem.*, 2018, **242**,
608 75–82.
609 43 T. de Souza Rocha, L. M. R. Hernandez, L. Mojica, M. H. Johnson, Y. K. Chang and E. González
610 de Mejía, Germination of Phaseolus vulgaris and alcalase hydrolysis of its proteins produced
611 bioactive peptides capable of improving markers related to type-2 diabetes in vitro, *Food Res. Int.*,
612 2015, **76**, 150-159.
613 44 L. M. Real Hernandez and E. Gonzalez de Mejia, Enzymatic Production, Bioactivity, and
614 Bitterness of Chickpea *(Cicer arietinum)* Peptides, *Compr. Rev. Food Sci. Food Saf.*, 2019, **18**,
615 1913–1946.
616 45 S. Chandrasekaran, D. Luna-Vital and E. G. de Mejia, Identification and Comparison of Peptides
617 from Chickpea Protein Hydrolysates Using Either Bromelain or Gastrointestinal Enzymes and

Their Relationship with Markers of Type 2 Diabetes and Bitterness, *Nutrients*, 2020, **12**, 3843.

46 M. F. Quintero-Soto, J. Chávez-Ontiveros, J. A. Garzón-Tiznado, N. Y. Salazar-Salas, K. V. Pineda-Hidalgo, F. Delgado-Vargas and J. A. López-Valenzuela, Characterization of peptides with antioxidant activity and antidiabetic potential obtained from chickpea *(Cicer arietinum* L,) protein hydrolysates, *J. Food Sci.*, 2021, 86, 2962-2977.

47 D. Röhrborn, N. Wronkowitz and J. Eckel, DPP4 in diabetes, *Front. Immunol.*, 2015, **6**, 386.

48 C. Lammi, C. Zanoni, A. Arnoldi and G. Vistoli, Peptides Derived from Soy and Lupin Protein as Dipeptidyl-Peptidase IV Inhibitors: *In Vitro* Biochemical Screening and *in Silico* Molecular Modeling Study, *J. Agric. Food Chem.*, 2016, **64**, 9601–9606.

49 F. Wang, Y. Zhang, T. Yu, J. He, J. Cui, J. Wang, X. Cheng and J. Fan, Oat globulin peptides regulate antidiabetic drug targets and glucose transporters in Caco-2 cells, *J. Funct. Foods*, 2018, **42**, 12-20.

50 C. Deacon, Metabolism of GIP and the contribution of GIP to the glucose-lowering properties of DPP-4 inhibitors, *Peptides*, 2020, **125**, 170196.

51 C. Proença, A. T. Rufino, J. M. P. Ferreira De Oliveira, M. Freitas, P. A. Fernandes, A. M. S. Silva and E. Fernandes, Inhibitory activity of flavonoids against human sucrase-isomaltase (α-glucosidase) activity in a Caco-2/TC7 cellular model, *Food Funct.*, 2022, **13**, 1108–1118.

52 T. T. Huang, P. P. Gu, T. Zheng, L. S. Gou and Y. W. Liu, Piperine, as a TAS2R14 agonist, stimulates the secretion of glucagon-like peptide-1 in the human enteroendocrine cell lines Caco-2, *Food Funct.*, 2022, **13**, 242–254.

53 R. Rasoamanana, N. Darcel, G. Fromentin and D. Tomé, Nutrient sensing and signalling by the gut, *Proc. Nutr. Soc.*, 2012, **71**, 446–455.

54 Q. Wang, K. I. Liszt, E. Deloose, E. Canovai, T. Thijs, R. Farré, L. J. Ceulemans, M. Lannoo, J. Tack and I. Depoortere, Obesity alters adrenergic and chemosensory signaling pathways that regulate ghrelin secretion in the human gut, *FASEB J.*, 2019, **33**, 4907–4920.

643 Figure Legends

644 **Figure 1**. **A**. SDS-PAGE of chickpea protein isolate. Lanes 1 and 2: protein isolate from
645 chickpeas soaked for 24 h; lanes 3 and 4: protein isolate from chickpeas germinated for
646 2 days; lanes 5 and 6: protein isolate from chickpeas germinated for 4 days; lanes 7 and 8:
647 protein isolate from chickpeas germinated for 6 days. A: Legumin J (18–24 kDa); B:
648 Legumin J (32–41 kDa); C: Lectins (43–45 kDa); D: Convicilin (50–54 kDa); E: Vicilin (59–
649 66 kDa); F: Convicilin (97–101 kDa); G: Legumin (105–109 kDa); H: Convicilin (110–
650 115 kDa); I: Legumin (136–139 kDa); J: Provicilin (149–151 kDa); K: Legumin (161–
651 169 kDa). **B**. Analysis of storage proteins in chickpea protein isolates from different days of
652 germination. Letters indicate significant differences with $p < 0.05$. Error bars indicate
653 standard of deviation. **C**. SDS-PAGE profile of 6-day germinated chickpea protein and 6-day
654 germinated protein hydrolysate. GCPH produced using ficin retains 50% of legumins from
655 protein isolate from chickpeas germinated for 6 days. Lanes 1 and 2: Chickpea protein isolate
656 from 6-day germinated chickpea; lanes 3 and 4: Chickpea protein hydrolysate produced using
657 6-day germinated protein and ficin at 1:10 E/S Ratio, 30 min hydrolysis time; **D**. Analysis of
658 changes to storage proteins after enzymatic hydrolysis with ficin.

659 **Figure 2**. **A**. Best pose of chickpea peptide FDLPAL in molecular docking studies with
660 DPP-IV; **B**. Position of chickpea peptide FDLPAL in molecular docking studies with DPP-
661 IV; **C**. Best pose of chickpea peptide VVFW in molecular docking studies with DPP-IV; **D**.
662 Position of chickpea peptide VVFW in molecular docking studies with DPP-IV; **E**. Best pose
663 of chickpea peptide GEAGR, with an energy of affinity of -8.3 kcal/mol, in the molecular
664 docking of the interaction with DPP-IV; **F**. Position of peptide GEAGR in the interaction
665 with DPP-IV. The positive control, vildagliptin, had an energy of affinity of -7.4 kcal/mol.
666 Bonding type: Neon green, conventional hydrogen bond; Light green: van der Waals; Pale
667 green, carbon hydrogen bond or Pi-donor hydrogen bond; Light Pink, Pi-alkyl bond; Purple,

668 Pi-sigma bond; Dark Pink, Pi-Pi T-shaped interactions; Red, Unfavorable interactions. **G**.
669 Biochemical DPP-IV inhibition by GCPH (IC_{50} 370 μM); **H**. DPP-IV inhibition in Caco-2
670 cells treated with GCPH for 24 h and stimulated with 30 mM glucose (IC_{50} 2100 μM);
671 **Figure 3. A**. Best pose of chickpea peptide FDLPAL, with an energy of affinity of -7.3
672 kcal/mol, in the molecular docking of the interaction with SI.; **B**. Position of peptide
673 FDLPAL in the interaction with SI; **C**. Best pose of chickpea peptide VVFW in molecular
674 docking studies with sucrase-isomaltase (SI); **D**. Position of chickpea peptide VVFW in
675 molecular docking studies with SI; **E**. Best pose of chickpea peptide GEAGR in molecular
676 docking studies with SI; **F**. Position of chickpea peptide GEAGR in molecular docking
677 studies with SI. The positive control, kotalanol, had an energy of affinity of -6.1 kcal/mol.
678 Bonding type: Neon green, conventional hydrogen bond; Light green: van der Waals; Pale
679 green, carbon hydrogen bond or Pi-donor hydrogen bond; Light Pink, Pi-alkyl bond; Purple,
680 Pi-sigma bond; Dark Pink, Pi-Pi T-shaped interactions; Red, Unfavorable interactions. **G**.
681 Biochemical α-glucosidase inhibition by GCPH (IC_{50} 190 μM); **H**. Inhibition of sucrase
682 activity in Caco-2 cells treated with GCPH and further stimulated with 20 mM sucrose.
683 **Figure 4**. **A**. Best pose of chickpea peptide FDLPAL in molecular docking studies with
684 SGLT1; **B**. Position of chickpea peptide FDLPAL in molecular docking studies with SGLT1
685 **C**. Best pose of chickpea peptide VVFW, with an energy of affinity of -9.9 kcal/mol, in
686 molecular docking studies of the interaction with SGLT1; **D**. Position of chickpea peptide
687 VVFW in the interaction with SGLT1. **E**. Best pose of chickpea peptide GEAGR in
688 molecular docking studies with SGLT1; **F**. Position of chickpea peptide GEAGR in
689 molecular docking studies with SGLT1. The positive control (phlorizin) had an affinity of -
690 9.1 kcal/mol. Bonding type: Neon green, conventional hydrogen bond; Light green: van der
691 Waals; Pale green, carbon hydrogen bond or Pi-donor hydrogen bond; Light Pink, Pi-alkyl

692 bond; Purple, Pi-sigma bond; Dark Pink, Pi-Pi T-shaped interactions, Red, Unfavorable
693 interactions.

694 **Figure 5**. **A.** Best pose of chickpea peptide FDLPAL in molecular docking studies with
695 GLUT2; **B**. Position of chickpea peptide FDLPAL in molecular docking studies with GLUT2
696 **C**. Best pose of chickpea peptide VVFW, with an energy of affinity of -10.0 kcal/mol, in
697 molecular docking studies of the interaction with GLUT2 ; **D**. Position of chickpea peptide
698 VVFW in the interaction with GLUT2; **E**. Best pose of chickpea peptide GEAGR in
699 molecular docking studies with GLUT2; **F**. Position of chickpea peptide GEAGR in
700 molecular docking studies with GLUT2; Positive control (phloretin) had an energy of affinity
701 of -8.4 kcal/mol. Bonding type: Neon green, conventional hydrogen bond; Light green: van
702 der Waals; Pale green, carbon hydrogen bond or Pi-donor hydrogen bond; Light Pink, Pi-
703 alkyl bond; Purple, Pi-sigma bond; Dark Pink, Pi-Pi T-shaped interactions, Red, Unfavorable
704 interactions.

705 **Figure 6**. **A**. Glucose uptake in Caco-2 cells treated with GCPH; **B**. Glucose uptake in
706 Caco-2 cells treated with pure peptides FDLPAL, GEAGR, and VVFW. **C.** SGLT1
707 expression in Caco-2 cells treated with GCPH; **D**. SGLT1 expression in Caco-2 cells treated
708 with pure peptides FDLPAL, GEAGR and VVFW. **E**. GLUT2 expression in Caco-2 cells
709 treated with GCPH. **F**. GLUT2 expression in Caco-2 cells treated with pure peptides
710 FDLPAL, GEAGR, and VVFW. Lanes 1: Non-treated cells, Lane 2: Phloretin (100 μM),
711 Lane 3: FDLPAL (50 μM), Lane 4: FDLPAL (100 μM), Lane 5: FDLPAL (250 μM), Lane 6:
712 GEAGR (50 μM), Lane 7: GEAGR (100 μM), Lane 8: GEAGR (250 μM), Lane 9: VVFW
713 (50 μM), Lane 10: VVFW (100 μM), Lane 11: VVFW (250 μM). A representative image of
714 the western blot is shown on top of the respective graph. Letters indicate significant
715 difference at $p < 0.05$. Bars indicate mean value obtained and error bars show standard
716 deviation.

717 **Figure 7**. **A**. Best pose of chickpea peptide FDLPAL in molecular docking studies with
718 T2R4; **B**. Position of chickpea peptide FDLPAL in molecular docking studies with T2R4; **C**.
719 Best pose of chickpea peptide VVFW in molecular docking studies with T2R4; **D**. Position of
720 chickpea peptide VVFW in molecular docking studies with T2R4; **E**. Best pose of peptide
721 GEAGR in molecular docking studies with T2R4; **F.** Position of peptide GEAGR in
722 molecular docking with T2R4; Bonding type: Neon green, conventional hydrogen bond;
723 Light green: van der Waals; pale green, carbon hydrogen bond or Pi-donor hydrogen bond;
724 Pink, Pi-alkyl bond; Purple, Pi-sigma bond.

725 **Figure 8**. **A**. Best pose of chickpea peptide FDLPAL in molecular docking studies with
726 T2R14; **B**. Position of chickpea peptide FDLPAL in molecular docking studies with T2R14;
727 **C**. Best pose of chickpea peptide VVFW in molecular docking studies with T2R14; **D**.
728 Position of chickpea peptide VVFW in molecular docking studies with T2R14; **E**. Best pose
729 of peptide GEAGR in molecular docking studies with T2R14; **F.** Position of peptide GEAGR
730 in molecular docking with T2R14; Bonding type: Neon green, conventional hydrogen bond;
731 Light green: van der Waals; pale green, carbon hydrogen bond or Pi-donor hydrogen bond;
732 Pink, Pi-alkyl bond; Purple, Pi-sigma bond.

733 **Figure 9**. Expression of bitter taste receptors and markers in Caco-2 cells treated with
734 GCPH. **A**. Expression of bitter taste receptor T2R4; **B**. Expression of bitter taste receptor
735 T2R14; **C**. Expression of bitter signaling pathway marker PLCβ2; **D**. Expression of bitter
736 taste signaling pathway marker TRPM5 in Caco-2 cells treated with GCPH. NT: non-treated;
737 PHL: phloretin, FA: flufenamic acid; DB: denatonium benzoate. **E**. Expression of bitter taste
738 receptor T2R4 in Caco-2 cells treated with different peptides. Lanes 1: Denatonium benzoate
739 (100 μM), Lane 2: Non-treated cells, Lane 3: FDLPAL (50 μM), Lane 4: FDLPAL (100
740 μM), Lane 5: FDLPAL (250 μM), Lane 6: GEAGR (50 μM), Lane 7: GEAGR (100 μM),
741 Lane 8: GEAGR (250 μM), Lane 9: VVFW (50 μM), Lane 10: VVFW (100 μM), Lane 11:

742 VVFW (250 μM); **F**. Expression of bitter taste receptor T2R14 in Caco-2 cells treated with
743 different peptides. Lanes 1: Flufenamic acid (100 μM), Lane 2: Non-treated cells, Lane 3:
744 FDLPAL (50 μM), Lane 4: FDLPAL (100 μM), Lane 5: FDLPAL (250 μM), Lane 6:
745 GEAGR (50 μM), Lane 7: GEAGR (100 μM), Lane 8: GEAGR (250 μM), Lane 9: VVFW
746 (50 μM), Lane 10: VVFW (100 μM), Lane 11: VVFW (250 μM); **G**. Expression of bitter
747 signaling pathway marker PLCβ2 in Caco-2 cells treated with different peptides. Lanes 1:
748 Non-treated cells, Lane 2: Phloretin (100 μM), Lane 3: FDLPAL (50 μM), Lane 4: FDLPAL
749 (100 μM), Lane 5: FDLPAL (250 μM), Lane 6: GEAGR (50 μM), Lane 7: GEAGR (100
750 μM), Lane 8: GEAGR (250 μM), Lane 9: VVFW (50 μM), Lane 10: VVFW (100 μM), Lane
751 11: VVFW (250 μM); **H**. Expression of bitter taste signaling pathway marker TRPM5 in
752 Caco-2 cells treated with different peptides. Lanes 1: Denatonium benzoate (100 μM), Lane
753 2: Non-treated cells, Lane 3: FDLPAL (50 μM), Lane 4: FDLPAL (100 μM), Lane 5:
754 FDLPAL (250 μM), Lane 6: GEAGR (50 μM), Lane 7: GEAGR (100 μM), Lane 8: GEAGR
755 (250 μM), Lane 9: VVFW (50 μM), Lane 10: VVFW (100 μM), Lane 11: VVFW (250 μM);
756 A representative image of the western blot is shown on top of the respective graph. Letters
757 indicate significant difference at $p < 0.05$. Bars indicate mean value obtained and error bars
758 show standard deviation.
759
760
761

763 Figure 1.

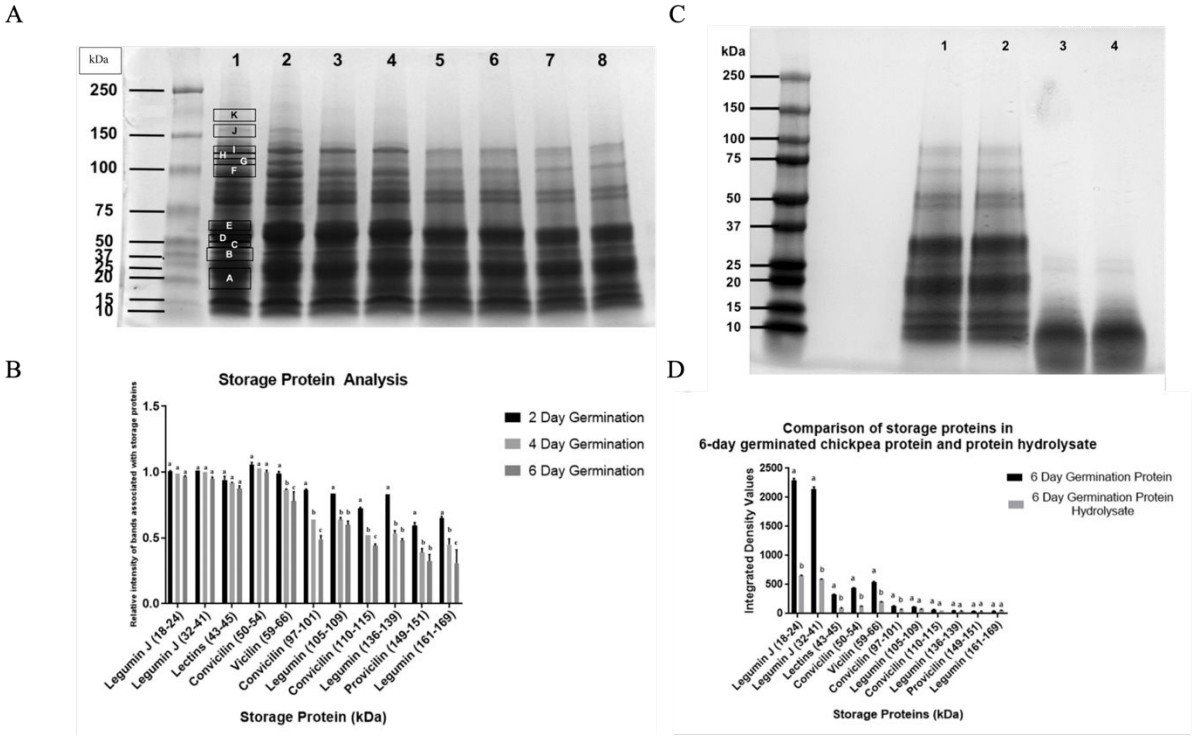

764
765

766 Figure 2.

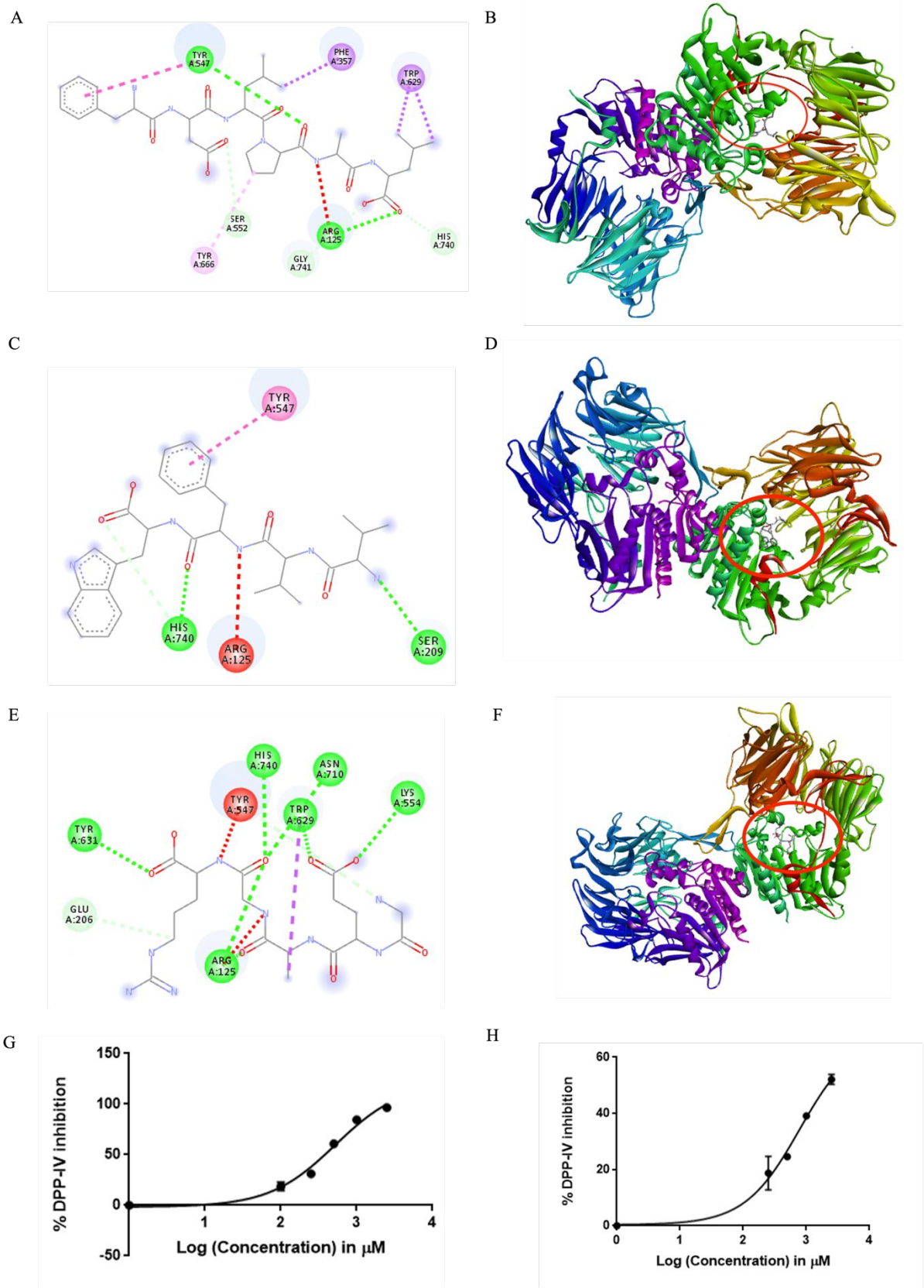

767
768

769 Figure 3.

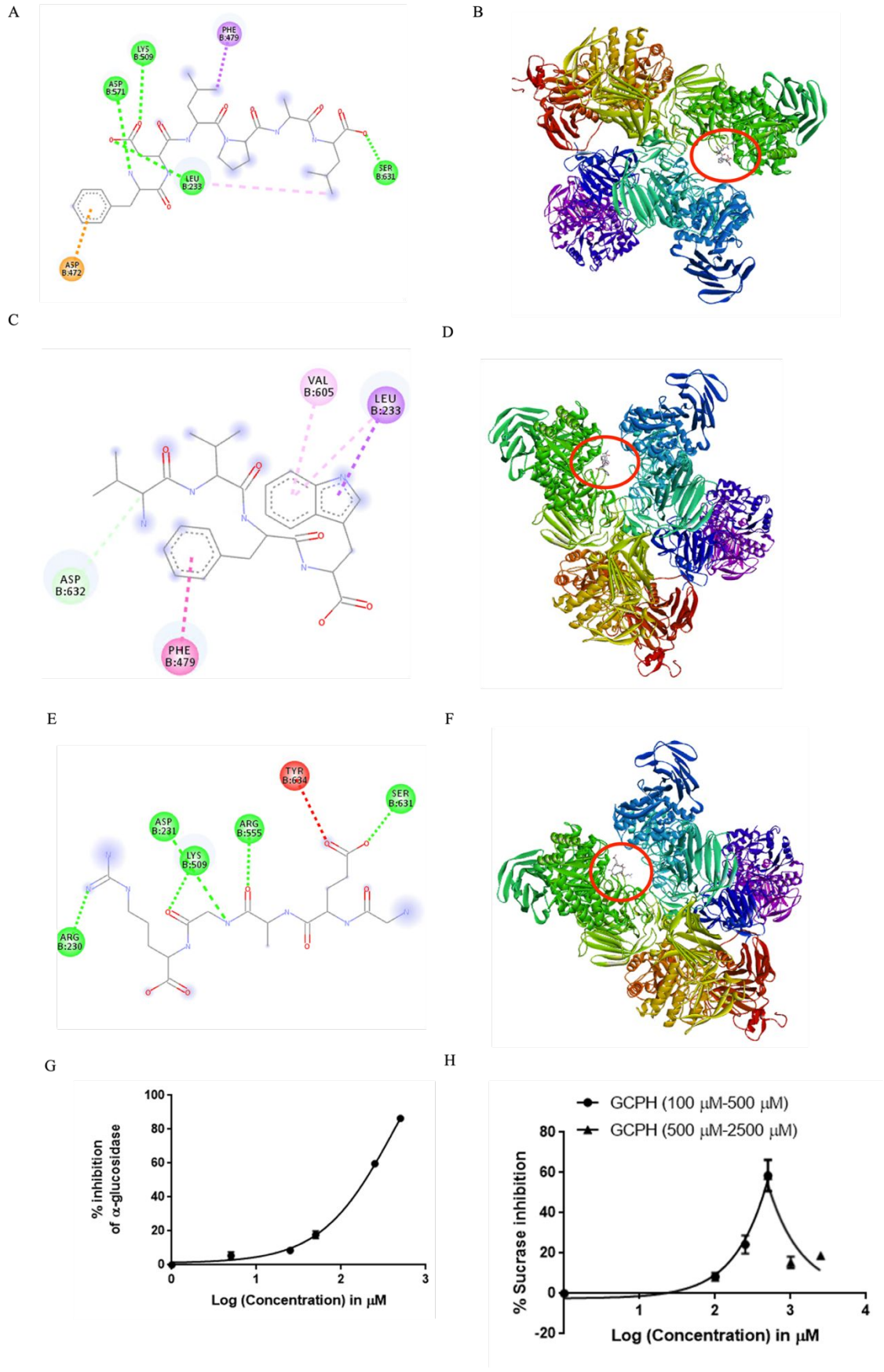

770

Figure 4.

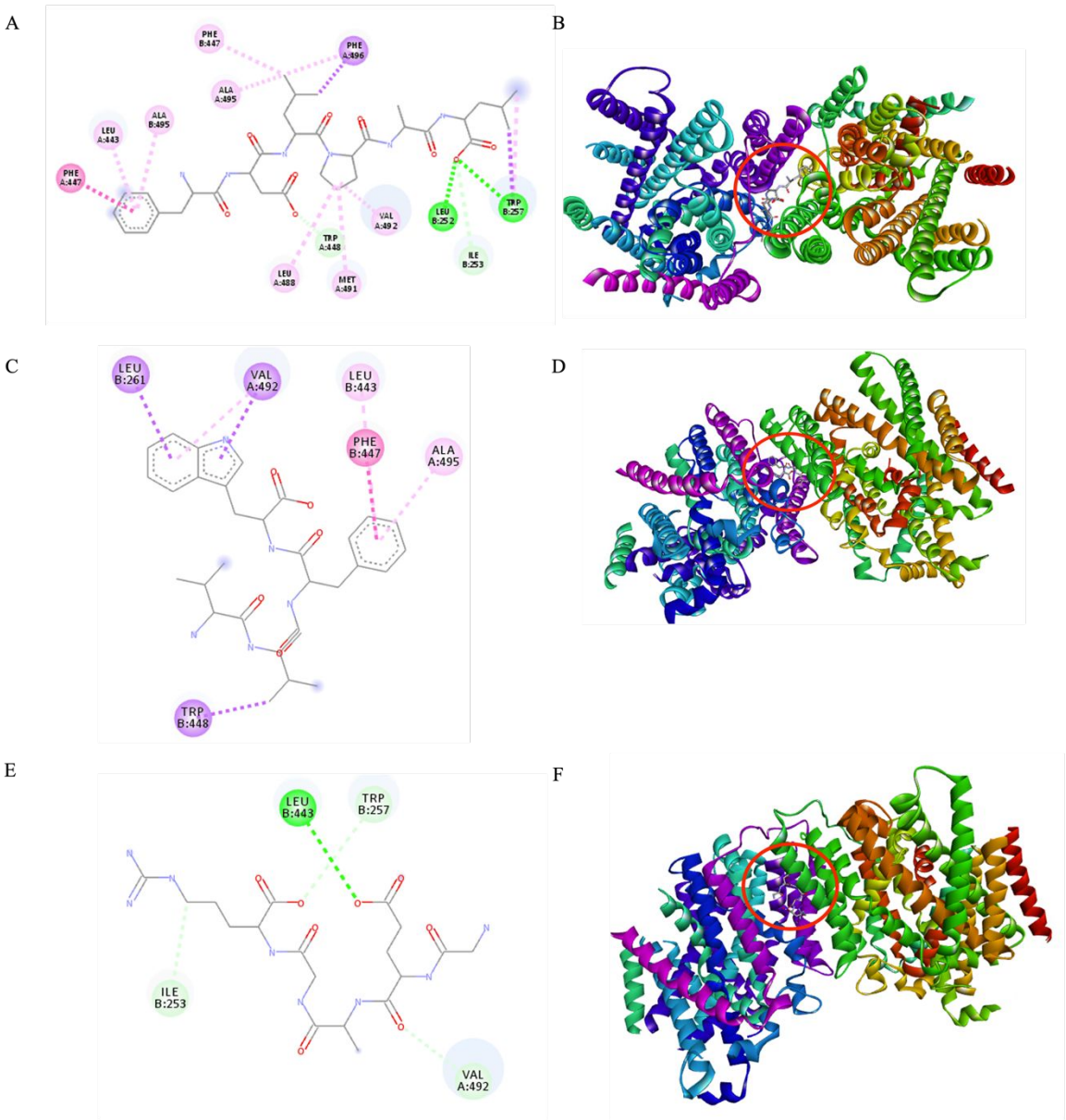
A
PHE B:447
PHE A:496
ALA A:495
LEU A:443
ALA B:495
PHE A:447
VAL A:492
LEU B:252
TRP B:257
TRP A:448
ILE B:253
LEU A:488
MET A:491
B
C
LEU B:261
VAL A:492
LEU B:443
PHE B:447
ALA A:495
TRP B:448
D
E
LEU B:443
TRP B:257
ILE B:253
VAL A:492
F

774 Figure 5.

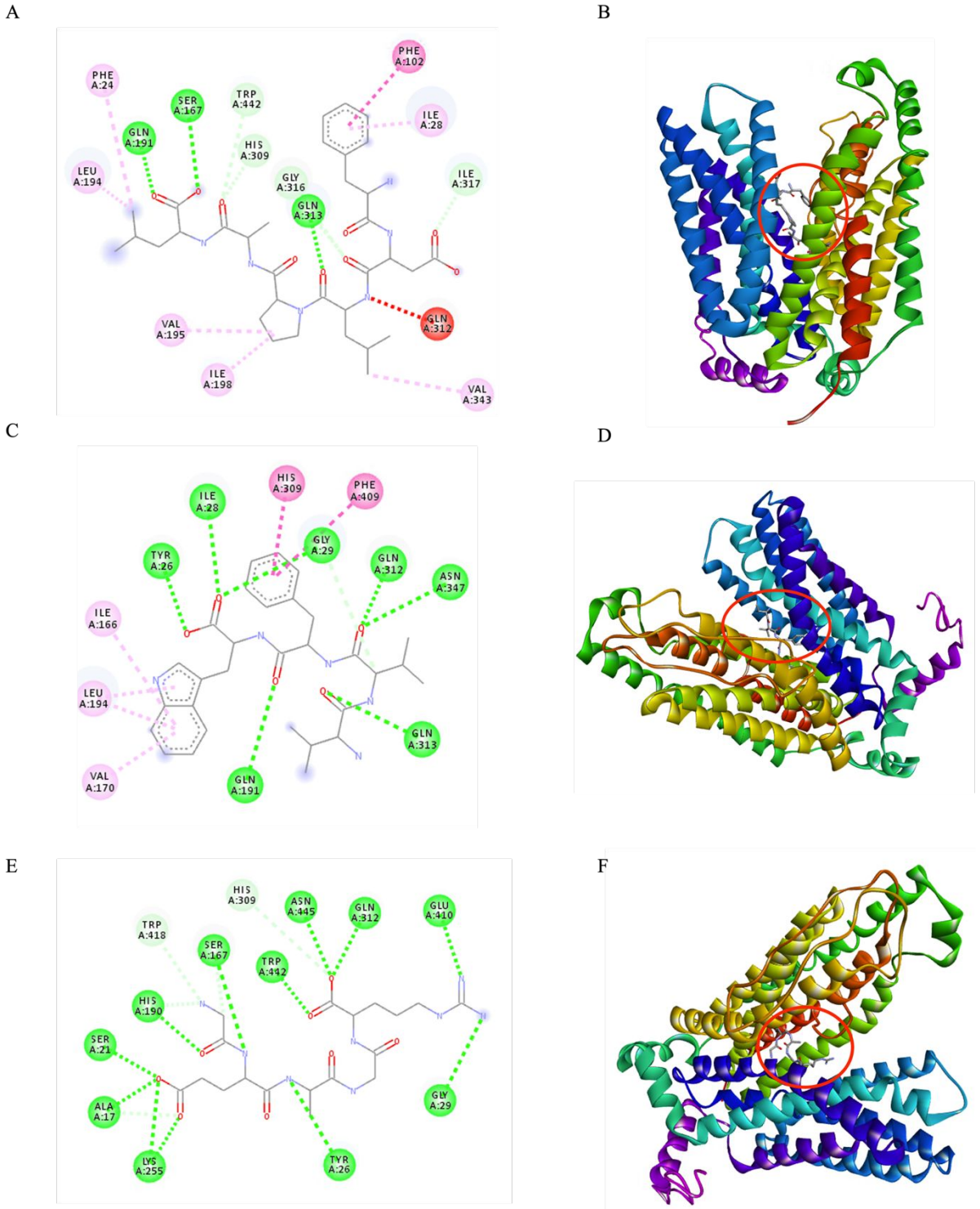

775
776

Figure 6.

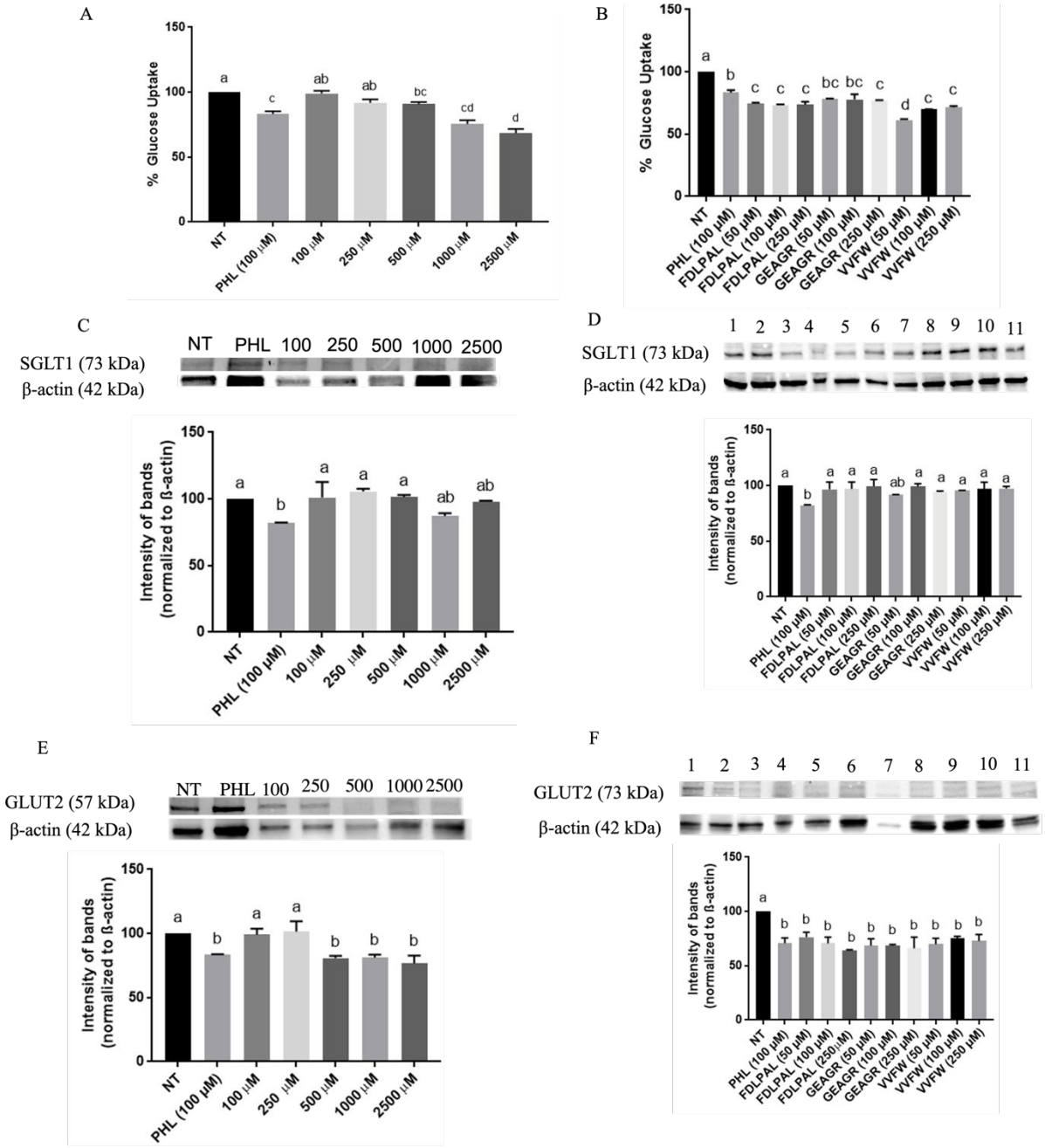
A
% Glucose Uptake
NT
PHL (100 µM)
100 µM
250 µM
500 µM
1000 µM
2500 µM
B
% Glucose Uptake
NT
PHL (100 µM)
FDLPAL (50 µM)
FDLPAL (100 µM)
FDLPAL (250 µM)
GEAGR (50 µM)
GEAGR (100 µM)
GEAGR (250 µM)
VVFW (50 µM)
VVFW (100 µM)
VVFW (250 µM)
C
NT PHL 100 250 500 1000 2500
SGLT1 (73 kDa)
β-actin (42 kDa)
Intensity of bands (normalized to ß-actin)
D
1 2 3 4 5 6 7 8 9 10 11
SGLT1 (73 kDa)
β-actin (42 kDa)
Intensity of bands (normalized to ß-actin)
E
NT PHL 100 250 500 1000 2500
GLUT2 (57 kDa)
β-actin (42 kDa)
Intensity of bands (normalized to ß-actin)
F
1 2 3 4 5 6 7 8 9 10 11
GLUT2 (73 kDa)
β-actin (42 kDa)
Intensity of bands (normalized to ß-actin)

780 Figure 7.

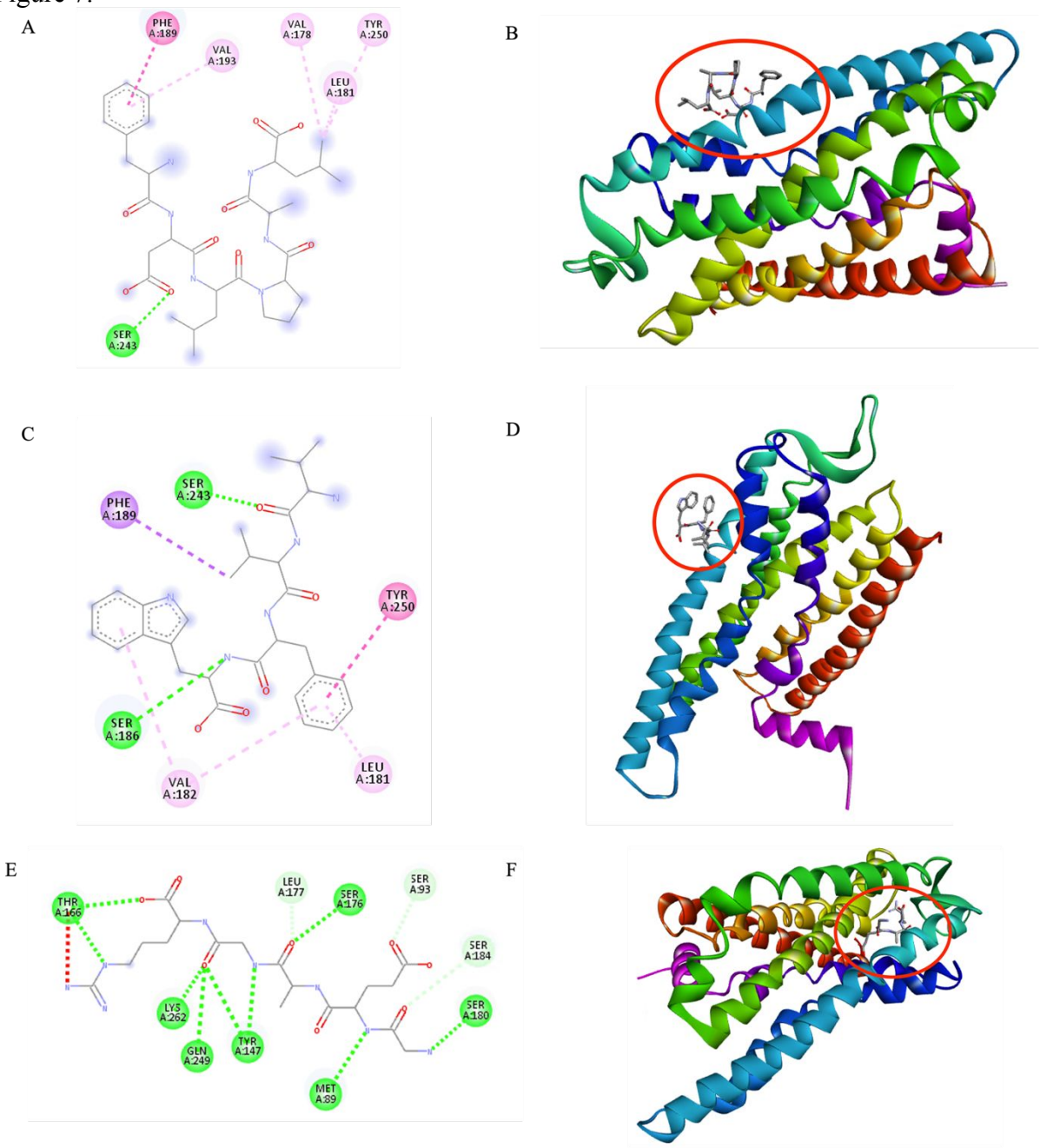

781
782

783 Figure 8.

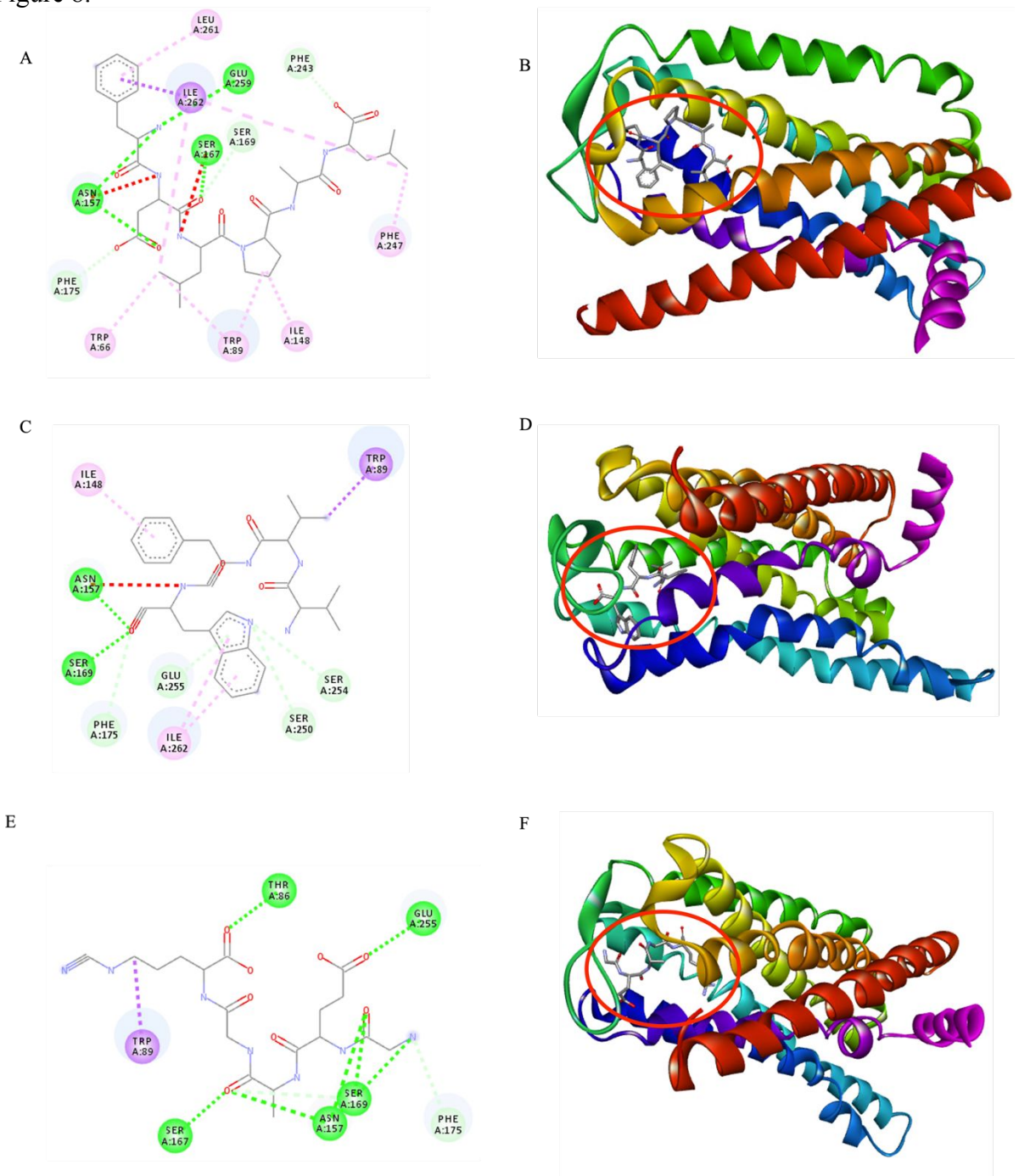

784
785

786 Figure 9.

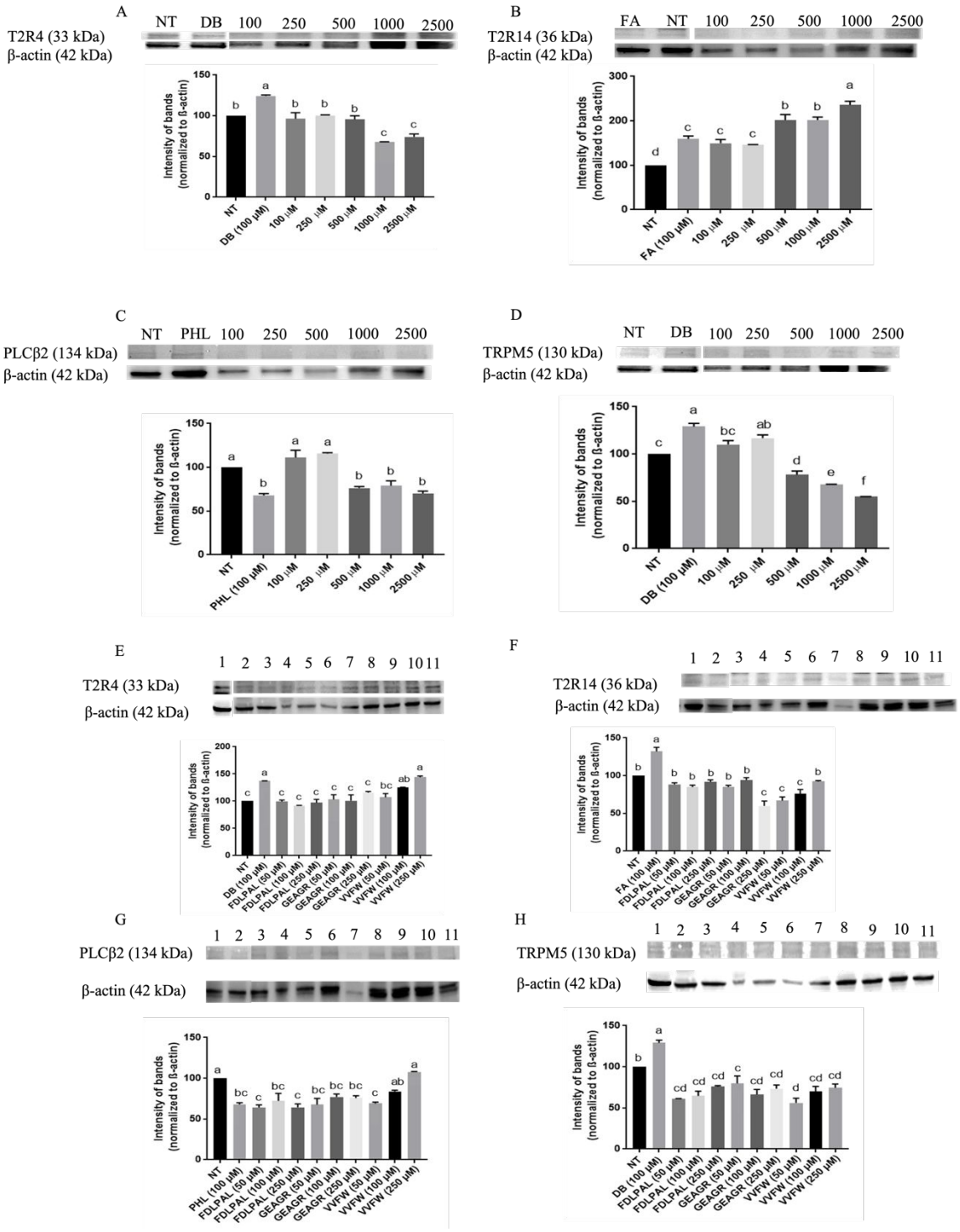

787

788 **Table 1**

789 Physicochemical, bioactive and bitter properties of peptides identified by LC-ESI-MS/MS from germinated chickpea protein ficin

790 hydrolysate from legumin.

Sequence	Mass (g/mol)	Isoelectric point	Net charge	Hydrophobicity (kcal/mol)	Bioactive properties	Associated peptide fragment	Bitter fragments	Activated Bitter Receptors
VVFW	549.3	5.69	0	3.18	ACE inhibitor	VF, VVF	F, VF, V, VV, FW, W	hTAS2R46, hTAS2R44, hTAS2R47, hTAS2R43, hTAS2R14, hTAS2R4, hTAS2R10, hTAS2R40, hTAS2R7, hTAS2R1, hTAS2R38, hTAS2R16, hTAS2R39, hTAS2R41, hTAS2R45, hTAS2R13, hTAS2R8, hTAS2R9
					DPP-IV inhibitor	VV, VF		
FDLPAL	674.4	3.12	-1	7.97	ACE inhibitor	DLP, LP	P, F, L, DL, PA	hTAS2R14, hTAS2R7, hTAS2R43, hTAS2R40, hTAS2R47, hTAS2R46, hTAS2R44, hTAS2R1, hTAS2R38, hTAS2R10, hTAS2R4, hTAS2R39, hTAS2R16, hTAS2R41, hTAS2R45, hTAS2R8
					DPP-IV inhibitor	PA, LP, AL		
GEAGR	488.2	6.85	0	16.14	ACE-inhibitor	AG, GR, GE, EA	R, GR, GE, EA	hTAS2R1, hTAS2R16, hTAS2R14, hTAS2R41, hTAS2R39, hTAS2R10
					DPP-IV inhibitor	AG, GE		
					α-Glucosidase inhibitor	EA		

792 **Table 2**

793 Molecular docking of peptides identified by LC-ESI-MS/MS from germinated chickpea protein ficin hydrolysate present in legumin.

794

	DPP-IV		Sucrase-Isomaltase		SGLT1		GLUT2	
Peptide	Energy of Affinity (kcal/mol)	Amino acid residues	Energy of Affinity (kcal/mol)	Amino acid residues	Energy of Affinity (kcal/mol)	Amino acid residues	Energy of Affinity (kcal/mol)	Amino acid residues
VVFW	-7.4	ARG125 [2.80], HIS740 [2.51, 3.53], SER209 [3.07], TYR547 [4.94]	-6.7	ASP632 [3.58], LEU233 [3.97, 5.00], PHE479 [3.82], VAL605 [4.28]	-9.9	ALA495 [4.43], LEU261 [3.60], LEU443 [5.45], PHE447 [4.09], TRP448 [3.60], VAL492 [3.58, 4.43]	-10.0	ASN347 [2.77], GLN191 [2.61], GLN312 [2.52], GLN313 [2.73], GLY29 [3.23], HIS309 [4.09], ILE28 [3.05], ILE166 [5.37], LEU194 [4.82, 5.04], PHE409 [4.92], TYR26 [3.17], VAL170 [5.26]
FDLPAL	-8.2	ARG125 [3.14, 3.39], GLY741 [3.55], HIS740 [3.52], PHE357 [3.73], SER552 [3.76], TRP629 [3.75, 3.81, 4.65], TYR547 [2.74, 4.35], TYR666 [4.75]	-7.3	ASP472 [3.91], ASP571 [3.31], LEU233 [2.24, 4.31], LYS509 [2.72], PHE479 [3.84], SER631 [1.88]	-9.8	LEU252 [2.89], LEU443 [5.42], LEU488 [4.35], MET491 [4.57], PHE447 [4.98], PHE496 [3.67, 4.15], TRP257 [3.67, 4.85], TRP448 [4.11], VAL492 [5.27]	-9.6	GLN191 [2.93], GLN312 [2.53], GLN313 [2.30, 2.63, 2.65], GLY316 [2.33], HIS309 [2.26], ILE28 [5.15], ILE198 [4.79], ILE317 [2.25], LEU194 [4.72], PHE24[5.34], PHE102 [4.53], SER167 [3.12], VAL195 [4.79], VAL343 [5.25]
GEAGR	-8.3	ARG125 [2.12, 2.16, 2.46], ASN710 [2.92], GLU206 [3.58], HIS740 [2.44], LYS554 [2.96], TRP629 [2.11, 3.82], TYR631 [2.82]	-5.1	ARG230 [2.86], ARG555 [2.74], ASP231 [3.30], LYS509 [1.95], SER631 [1.97], TYR634 [2.98]	-6.9	ILE253 [3.57], LEU443 [3.24], TRP257 [3.72, 4.13], VAL492 [3.43]	-7.3	ALA17 [2.62, 3.16], ASN445 [3.05], GLN372 [2.88], GLU410 [3.34], GLY29 [3.32], HIS190 [2.17, 3.09], HIS309 [3.68], LYS255 [2.17, 3.06], SER21 [2.79], SER167 [3.21, 3.71], TRP418 [3.90], TRP442 [1.96], TYR26 [3.14]

796 **Table 3** Summary of biochemical DPP-IV and α-glucosidase inhibition, and *in vitro* glucose uptake, DPP-IV and sucrase-isomaltase

797 inhibition in Caco-2 cells. GCPH: germinated chickpea protein hydrolysate, DPP-IV: Dipeptidyl peptidase-IV

Sample	Biochemical			Caco-2 cells			
	DPP-IV (%)	α-glucosidase (%)	Glucose Uptake (%)	DPP-IV in cell media (%)	Sucrase inhibition (%)	Maltase inhibition (%)	Isomaltase inhibition (%)
NT	0 ± 0.45 a	0 ± 0.12 a	0 ± 0.30 a	0.00 ± 3.68 a	0 ± 2.14 a	0 ± 1.41 a	0 ± 1.76 a
Positive Control	99.53 ± 0.81 (Sitagliptin 100 µM)	38.24 ± 6.95 (Acarbose 2000 µM)	16.67 ± 1.97 (Phloretin 100 µM) b	97.34 ± 0.08 (Sitagliptin 500 µM) f	25.71 ± 1.33 (Acarbose 2000 µM) cde	74.80 ± 0.16 (Acarbose 2000 µM) g	39.11 ± 1.92 (Acarbose 2000 µM) d
FDLPAL (50 µM)	0 ± 1.35 a	0 ± 0.002 a	25.21 ± 0.49 c	5.53 ± 1.72 ab	17.74 ± 1.41 bc	63.42 ± 7.44 f	51.88 ± 0.59 g
FDLPAL (100 µM)	8.83 ± 1.44 b	0 ± 0.003 a	26.76 ± 0.71c	5.92 ± 1.27 ab	44.11 ± 4.81 g	64.17 ± 1.50 gh	48.31 ± 1.15 fg
FDLPAL (250 µM)	11.45 ± 0.45 bc	0 ± 0.005 a	26.15 ± 2.14 c	5.72 ± 0.25 ab	22.78 ± 3.77 bcd	33.20 ± 1.26 cd	34.33 ± 3.35 e
GEAGR (50 µM)	0 ± 1.62 a	0 ± 0.004 a	21.87 ± 0.57 bc	0.00 ± 0.99 a	33.18 ± 0.63 ef	59.59 ± 1.63 f	46.37 ± 1.49 ef
GEAGR (100 µM)	10.54 ± 0.09 b	0 ± 0.001 a	22.12 ± 4.04 bc	5.33 ± 0.62 ab	29.20 ± 1.44 de	57.33 ± 1.21 f	46.39 ± 0.75 ef
GEAGR (250 µM)	11.14 ± 0.99 b	0 ± 0.003 a	23.26 ± 0.62 b	4.92 ± 1.42 ab	18.50 ± 0.97 bc	46.44 ± 1.49 f	49.88 ± 0.49 fg
VVFW (50 µM)	0 ± 2.62 a	0 ± 0.048 a	38.68 ± 0.83 d	0.00 ± 1.29 a	21.01 ± 2.27 bc	0 ± 1.03 a	0.25 ± 0.35 a
VVFW (100 µM)	7.97 ± 0.90 b	9.21 ± 1.12 bc	30.22 ± 0.19 c	4.07 ± 2.50 ab	19.69 ± 0.66 bcd	0 ± 0.77 a	18.44 ± 0.79 b

VVFW (250 μM)	9.65 ± 2.98 b	20.26 ± 5.58 c	28.59 ± 1.09 c	4.29 ± 0.79 ab	39.33 ± 2.12 f	12.54 ± 1.11 b	35.79 ± 1.47 d
GCPH (100 μM)	18.81 ± 4.15 c	5.68 ± 1.61 ab	0.99 ± 2.08 ab	9.56 ± 0.64 b	8.42 ± 2.06 a	0 ± 0.43 a	0.00 ± 0.01 a
GCPH (250 μM)	31.26 ± 0.99 d	8.79 ± 0.45 ab	8.21 ± 2.67 ab	18.78 ± 5.94 c	24.38 ± 4.52 bcde	28.90 ± 2.63 c	67.88 ± 4.51 h
GCPH (500 μM)	60.94 ± 1.44 e	18.09 ± 1.61 c	9.16 ± 1.56 bc	24.65 ± 0.64 c	58.52 ± 7.78 h	39.87 ± 7.85 de	64.88 ± 3.21 h
GCPH (1000 μM)	84.51 ± 3.14 f	59.95 ± 0.90 d	24.43 ± 2.89 cd	39.13 ± 0.02 d	15.47 ± 2.89 b	46.30 ± 2.70 e	23.62 ± 3.13 b
GCPH (2500 μM)	96.62 ± 0.99 g	86.82 ± 1.34 e	31.58 ± 3.29 d	52.12 ± 1.73 e	18.77 ± 0.61 bc	38.31 ± 2.28 c	29.2 ± 2.39 b

Table 4. Correlation plot showing R values between markers of T2D tested in Caco-2 cells.

	Biochemical DPP-IV inhibition	Biochemical α-glucosidase inhibition	DPP-IV inhibition *in vitro*	Sucrase inhibition	Maltase inhibition	Isomaltase inhibition	Glucose Uptake	SGLT 1	GLUT 2	TAS2R 4	TAS2R 14	PLC β2	TRPM5
Biochemical DPP-IV inhibition	1												
Biochemical α-glucosidase inhibition	0.91*	1											
DPP-IV inhibition *in vitro*	0.99*	0.93*	1										
Sucrase inhibition	0.09	-0.06	0.03	1									
Maltase inhibition	0.15	0.06	0.18	0.41	1								
Isomaltase inhibition	0.24	0.05	0.17	0.42	0.51*	1							
Glucose Uptake	0.01	0.22	0.04	0.18	0.2	0.22	1						
SGLT1	-0.12	-0.26	-0.09	0.09	-0.3	-0.41	-0.51*	1					
GLUT2	0.16	0.07	0.18	-0.4	-0.45	-0.48	-0.81*	0.5*	1				
T2R4	-0.66*	-0.52*	-0.68*	0.17	-0.38	-0.41	0.14	0.16	-0.2	1			
T2R14	0.94*	0.82*	0.93*	0.08	-0.06	0.16	-0.25	0.09	0.4	-0.67*	1		
PLCβ2	-0.05	-0.06	-0.06	-0.21	-0.57*	0.16	-0.62*	0.49	0.77*	0.32	0.12	1	
TRPM5	-0.15	-0.29	-0.29	-0.24	-0.38	-0.45	-0.86*	0.56*	0.8*	0.08	0.08	0.8*	1

Asterisks indicate significance value of $p < 0.05$. Increasing intensity of blue indicates stronger positive correlation and increasing intensity of orange indicates stronger negative correlation.